

Renormalized equations of motions for scalars and fermions in the 2PI formalism

A. Banik^{*}, H. Hinrichsen[†] and W. Porod[‡]

*Institut für Theoretische Physik und Astrophysik, Universität Würzburg,
D-97074 Würzburg, Germany*

Abstract

We present on shell-scheme for the 2PI formalism with a particular focus on the renormalized equations of motion. We first revisit the so-called Hartree approximation where we give the counterterms for both the broken and unbroken phase. Moreover, we give explicit formulas for the renormalized three- and four-point functions in the broken phase. We then turn to the sunset approximation, with only scalars and then including fermions. We give explicit formulas for the wavefunction and mass counterterms. Moreover, we show that, in particular, the two-point functions can be obtained numerically in a fast converging scheme even for large couplings of order one.

1 Introduction

The vast majority of physical phenomena, which are vital to our understanding of nature, take place out of equilibrium. Non-equilibrium processes can be found in a wide range of physical domains ranging from particle physics and cosmology to astrophysics and condensed matter systems. A few examples are heavy-ion collisions performed, for instance, at the Large Hadron Collider (LHC) with the aim to produce quark-gluon plasma, the generation of density fluctuations during inflation and the explosive particle production at the end of inflation, as well as phase transitions in the early universe or in condensed matter systems. These phenomena also go beyond the reach of standard perturbation theory, meaning one needs to resort to non-perturbative methods for consistent results.

The challenge of addressing models beyond perturbation theory and tackling out-of-equilibrium aspects can be fulfilled using functional integral techniques based on n -particle irreducible (n PI) effective actions. In this work, we focus on the two-particle irreducible

^{*}E-mail: amitayus.banik@uni-wuerzburg.de

[†]E-mail: hinrichsen@physik.uni-wuerzburg.de

[‡]E-mail: porod@physik.uni-wuerzburg.de

(2PI) formalism [1, 2], where the expectation value of the field (one-point function) and the propagator (two-point function) constitute the dynamical degrees of freedom.

Resummation schemes based on the 2PI effective action have been known to show better convergence properties in comparison to other methods, such as in bosonic finite temperature field theory [3–5] and inflationary preheating [6]. Out-of-equilibrium properties can be formally studied, whereby the resummation feature of the 2PI formalism allows one to obtain approximations uniform in time [7–10]. Furthermore, approximations within the 2PI formalism have been shown to be consistent with (global) conservation laws stemming from Noether’s theorem, thus guaranteeing charge and energy conservation [11, 12]. Finally, using the equations of motion of the 2PI formalism one can obtain, in principle, the transport equations [13, 14] which are an important ingredient in the study of cosmological phase transitions, see for e.g. [13, 15, 16].

By definition, approximation schemes based on the 2PI formalism involve resummation of the two-point function to all orders in perturbation theory, when one chooses a particular truncation for the expansion, such as restricting to a given loop order. Despite this selective resummation, 2PI methods show renormalizability through local counterterms, as demonstrated in [17–20] for a symmetric scalar theory with a quartic coupling. The procedure to obtain the counterterms for $O(N)$ symmetric theories has been explored in [21–25]. Progress has also been with regard to renormalizability with the inclusion of abelian gauge bosons and consistency with Ward identities [5, 26–29], as well as the inclusion of fermions [30]. A systematic approach for the renormalization of the 2PI action been presented in [31] focusing on scalars.

An aspect which has to our knowledge not been discussed so far is how to obtain an on-shell renormalization scheme for the 2PI formalism. Our aim is to obtain this for a coupled system of fermions and scalars. We will do this with a particular focus on the renormalized equations of motions which in turn, can be used as starting point for transport equations in cosmological phase transitions. In the present work, we demonstrate the applicability of the techniques in [31] to various truncations of the 2PI effective action at two-loop order, and extend the techniques to incorporate fermions in the 2PI formalism. Our main aim is to present the renormalized equations of motion, after which we focus on the necessary steps to obtain the various counterterms.

The paper is organized as follows: in Section 2, we first recall relevant features of the 2PI formalism, focusing in particular on obtaining the renormalized equations of motion. It is well-known that these equations contain several counterterms which need to be fixed by appropriate renormalization conditions. To this end, we present a suitable on-shell scheme in Section 3, which allows for connecting to physical observables in a straightforward fashion. We then apply this scheme to various two-loop truncations of the 2PI effective action. We start in Section 4 with the well-known Hartree approximation. We find, in particular, that all counterterms are finite and give explicit relations between the broken and unbroken phases for these counterterms. In the Hartree approximation, one can give analytic expressions for all interesting quantities, though this does not hold in other cases. Therefore, we proceed to the so-called scalar sunset approximation to demonstrate the intricacies and how to resolve them. This model also provides a simple example containing a so-called memory integral in

the equation of motion which are important for the thermalisation of a system, see e.g. [10]. Within this framework, we obtain the gap equation to obtain the renormalized two-point function and solve it using an iterative procedure. We demonstrate that this procedure converges very fast even for large couplings.

In Section 5, we take the fermionic sunset approximation, which serves as the simplest example to include fermions in the 2PI formalism. Here, we obtain coupled system of gap equations for the fermionic and scalar propagators which we again solve using the aforementioned iterative procedure, finding sufficiently fast convergence for an $\mathcal{O}(1)$ Yukawa coupling. We find that the inclusion of fermions renders none of the counterterms finite. Finally, in Section 6, we present our conclusions and give an outlook.

2 The 2PI Formalism and Renormalized Equations of Motion

In order to fix notation, let us first summarize some key aspects of the 2PI formalism in the example of a single scalar field [2], with the generating functional as starting point

$$Z[J_1, J_2] = \int \mathcal{D}\varphi \exp \left(iS[\varphi] + i \int_x J_1(x)\varphi(x) + \frac{i}{2} \int_{xy} \varphi(x)J_2(x, y)\varphi(y) \right), \quad (1)$$

where x and y denote vectors in a d -dimensional Minkowski space with the mostly minus signature and J_1 and J_2 are two external currents suitably shifted in order to account for a Gaussian initial state. Since one is interested in the non-equilibrium evolution, where a final state is not known, the temporal integration in

$$\int_x \equiv \int_{\mathcal{C}} dx_0 \int d^{d-1}x \quad (2)$$

is carried out along a time-ordered Keldysh contour \mathcal{C} . In terms of the cumulant-generating functional $W[J_1, J_2] = -i \ln Z[J_1, J_2]$, the macroscopic field and the connected two-point correlator, defined as $\phi(x) = \langle \varphi(x) \rangle_{\mathcal{C}}$ and $G(x, y) = \langle \varphi(x)\varphi(y) \rangle_{\mathcal{C}}$, are given by

$$\phi(x) = \frac{\delta W[J_1, J_2]}{\delta J_1(x)}, \quad G(x, y) = 2 \frac{\delta W[J_1, J_2]}{\delta J_2(x, y)} - \phi(x)\phi(y). \quad (3)$$

It is more practical to describe the system by the Legendre transform of $W[J_1, J_2]$, the so-called 2PI effective action

$$\Gamma^{2\text{PI}}[\phi, G] = W[J_1, J_2] - \int_x \frac{\delta W[J_1, J_2]}{\delta J_1(x)} J_1(x) - \int_{xy} \frac{\delta W[J_1, J_2]}{\delta J_2(x, y)} J_2(x, y) \quad (4)$$

$$= W[J_1, J_2] - \int_x \phi(x)J_1(x) - \frac{1}{2} \int_{xy} \left(\phi(x)\phi(y) + G(x, y) \right) J_2(y, x) \quad (5)$$

which allows the currents to be expressed as

$$J_1(x) = -\frac{\delta \Gamma^{2\text{PI}}[\phi, G]}{\delta \phi} - \int_y J_2(x, y)\phi(y), \quad J_2(x, y) = -2 \frac{\delta \Gamma^{2\text{PI}}[\phi, G]}{\delta G(x, y)}. \quad (6)$$

The effective action can be split into $\Gamma^{2\text{PI}}[\phi, G] = \Gamma_1^{2\text{PI}}[\phi, G] + \Gamma_2^{2\text{PI}}[\phi, G]$, where

$$\Gamma_1^{2\text{PI}}[\phi, G] = S[\phi] + \frac{i}{2}\text{Tr} [\ln G^{-1}] + \frac{i}{2}\text{Tr} [\tilde{G}_\phi^{-1}G] - \underbrace{\frac{i}{2}\text{Tr} [G^{-1}G]}_{=\text{const}} \quad (7)$$

comprises the classical action and all 1-loop contributions while $\Gamma_2^{2\text{PI}}[\phi, G]$ accounts for higher contributions from 2-loop onward. ‘‘Tr’’ refers to integration over the space-time variables. Here,

$$\tilde{G}_\phi^{-1} = -i \frac{\delta^2 S[\phi]}{\delta\phi(x)\delta\phi(y)} \quad (8)$$

denotes the classical inverse propagator and the trace stands for integration along the Keldysh contour. In practical calculations, $\Gamma_2^{2\text{PI}}[\phi, G]$ is only evaluated up to given loop order.

In view of the renormalization procedure, it is useful to split the action into a free and an interacting part $S[\phi] = S_0[\phi] + S_{\text{int}}[\phi]$ and to decompose $\tilde{G}_\phi^{-1} = \tilde{G}_0^{-1} + \tilde{G}_{\phi,\text{int}}^{-1}$ [31]. Correspondingly one can split the effective action into $\Gamma^{2\text{PI}} = \Gamma_0^{2\text{PI}} + \Gamma_{\text{int}}^{2\text{PI}}$, where

$$\Gamma_0^{2\text{PI}}[\phi, G] = S_0[\phi] + \frac{i}{2}\text{Tr} [\ln G^{-1}] + \frac{i}{2}\text{Tr}[\tilde{G}_0^{-1}G], \quad (9)$$

$$\Gamma_{\text{int}}^{2\text{PI}}[\phi, G] = S_{\text{int}}[\phi] + \frac{i}{2}\text{Tr}[\tilde{G}_{\phi,\text{int}}^{-1}G] + \Gamma_2[\phi, G] + \text{const}. \quad (10)$$

The stationarity conditions determine the physical one- and two-point functions $\bar{\phi}$ and \bar{G} in the absence of external sources. i.e. $J_1 = 0$ and $J_2 = 0$:

$$\left. \frac{\delta\Gamma^{2\text{PI}}[\phi, G]}{\delta\phi(x)} \right|_{\bar{\phi}, \bar{G}} = \left. \frac{\delta S_0[\phi, G]}{\delta\phi(x)} \right|_{\bar{\phi}} + \left. \frac{\delta\Gamma_{\text{int}}^{2\text{PI}}[\phi, G]}{\delta\phi(x)} \right|_{\bar{\phi}, \bar{G}} = 0, \quad (11)$$

$$\left. \frac{\delta\Gamma^{2\text{PI}}[\phi, G]}{\delta G(x, y)} \right|_{\bar{\phi}, \bar{G}} = -\frac{i}{2}\bar{G}^{-1}(x, y) + \frac{i}{2}\tilde{G}_0^{-1}(x, y) + \left. \frac{\delta\Gamma_{\text{int}}^{2\text{PI}}[\phi, G]}{\delta G(x, y)} \right|_{\bar{\phi}, \bar{G}} = 0. \quad (12)$$

We note for completeness that these conditions imply that the sources need to be redefined order-by-order once a perturbative evaluation is performed, as has already been pointed out in [1] in the context of usual 1PI effective action.

At this stage, it is useful to introduce the self-energy

$$\bar{\Pi}(x, y) = 2i \left. \frac{\delta\Gamma_{\text{int}}^{2\text{PI}}[\phi, G]}{\delta G(x, y)} \right|_{\bar{\phi}, \bar{G}} \quad (13)$$

which can be decomposed into a local part, proportional to $\delta_{\mathcal{C}}(x - y)$, and a non-local one, see below. The index \mathcal{C} indicates that the Delta-distribution takes values along the Keldysh contour.

The one- and two-point functions are obtained from the equations of motions (EOMs) once the corresponding boundary conditions are specified. More concretely, the EOM for ϕ

is given by eq. (11) whereas the one for the two point function can be obtained from eq. (12) by convoluting it with $G(y, z)$ yielding

$$(\square_x + m^2)G(x, z) + \int_y \bar{\Pi}(x, y)G(y, z) = \delta_C(x - z). \quad (14)$$

Fermions can be treated in an analogous way [2, 9]. We will denote the Dirac field by $\psi(x)$ and the corresponding two-point function by $D(x, y)$. With the assumption that the fermionic field does not acquire a vacuum expectation value (VEV), we obtain the generic equation of motion for $D(x)$ as

$$(\mathbf{i}\not{\partial} - M)D(x, z) + \int_y \bar{\Sigma}(x, y)D(y, z) = \delta_C(x - z), \quad (15)$$

where $\bar{\Sigma}(x, y)$ is the fermionic self-energy given by

$$\bar{\Sigma}(x, y) = \mathbf{i} \frac{\delta \Gamma_{\text{int}}^{2\text{PI}}[\phi, G, D]}{\delta D(x, y)} \Big|_{\bar{\phi}, \bar{G}, \bar{D}}. \quad (16)$$

Later, we will renormalize the fields based on a procedure that we will outline, retaining the assumption that ψ does not get a VEV.

We take the following classical action as a starting point

$$\begin{aligned} S[\phi, \psi] &= S_0[\phi, \psi] + S_{\text{int}}[\phi, \psi] \\ &= \int_x \left\{ \frac{1}{2} \partial_\mu \phi(x) \partial^\mu \phi(x) - \frac{m^2}{2} \phi^2(x) + \bar{\psi}(x) (\mathbf{i}\not{\partial} - M) \psi(x) \right. \\ &\quad \left. - \frac{\alpha}{3!} \phi^3(x) - \frac{\lambda}{4!} \phi^4(x) - g \bar{\psi}(x) \psi(x) \phi(x) \right\} \end{aligned} \quad (17)$$

where in the last step we have split the action into a free and an interaction part corresponding to the first and second line of (18). We will include all contributions of the effective action up to two-loop order which is sufficient to detail all the intricacies of the renormalization, in particular in the fermionic sector. The 2PI action up to this order is given by

$$\begin{aligned} \Gamma_{2\text{PI}}[\phi, G, D] &= \int_x \left\{ \frac{1}{2} \partial_\mu \phi(x) \partial^\mu \phi(x) - \frac{m^2}{2} \phi^2(x) - \frac{\alpha}{3!} \phi^3(x) - \frac{\lambda}{4!} \phi^4(x) \right. \\ &\quad \left. - \frac{1}{2} (\square_x + m^2) G(x, y) \Big|_{x=y} - \frac{1}{2} \alpha \phi(x) G(x, x) - \frac{1}{8} \lambda G^2(x, x) - \frac{1}{4} \lambda \phi^2(x) G(x, x) \right. \\ &\quad \left. + \text{tr} \left[(\mathbf{i}\not{\partial}_x - M) D(x, y) \Big|_{x=y} \right] - g \phi(x) \text{tr}[D(x, x)] \right\} \\ &\quad + \int_x \int_y \left[\frac{\mathbf{i}}{12} (\alpha + \lambda \phi(x)) (\alpha + \lambda \phi(y)) G^3(x, y) - \frac{\mathbf{i}}{2} g^2 G(x, y) \text{tr}[D(x, y) D(y, x)] \right]. \end{aligned} \quad (19)$$

where we have already used the fact that terms linear in ψ vanish as it does not acquire a VEV. We note for completeness, that the last line will give rise to the so-called “memory integrals”. We stress that (19) represents the unrenormalized action and that (11), (14) and (15) hold for both the unrenormalized and renormalized action.

Eventually, we are interested in obtaining the renormalized EOMs. It has been shown in [31] that one needs not only to renormalize the couplings appearing in the classical action S but also the ones which couple one-point functions to two-point functions, as well as the couplings between two-point functions only. The reason is, that the two-point functions are resummed propagators within the 2PI formalism implying orders in perturbation theory get mixed. However, it has been shown on general grounds in ref. [31], that this is done in a particular way. This allows one to carry out the renormalization such that only a finite number of counterterms are needed.

As is customary, we first define the renormalized fields from the bare ones, using their respective wave-function renormalizations, as

$$\begin{aligned}\phi(x) &= Z_{\phi,2}^{\frac{1}{2}}\phi_R(x), & G(x,y) &= Z_{\phi,0}G_R(x,y), \\ \psi(x) &= Z_{\psi,2}^{\frac{1}{2}}\psi_R(x), & D(x,y) &= Z_{\psi,0}D_R(x,y),\end{aligned}\tag{20}$$

where we have indicated the number of fields ϕ (ψ) associated with a term by the index i in $Z_{\phi,i}$ ($Z_{\psi,i}$). We adopt this same notation for the mass and coupling counterterms, and obtain

$$\begin{aligned}Z_{\phi,2}m^2 &= m_R^2 + \delta m_2^2, & Z_{\phi,2}^{\frac{i}{2}}Z_{\phi,0}^{\frac{3-i}{2}}\alpha &= \alpha_R + \delta\alpha_i \quad (i = 0, 1, 3) \\ Z_{\phi,0}m^2 &= m_R^2 + \delta m_0^2, & Z_{\phi,2}^{j/2}Z_{\phi,0}^{(4-j)/2}\lambda &= \lambda_R + \delta\lambda_j \quad (j = 0, 2, 4), \\ Z_{\psi,0}M &= M_R + \delta M_0, & Z_{\psi,0}Z_{\phi,2}^{\frac{k}{2}}Z_{\phi,0}^{\frac{1-k}{2}}g &= g_R + \delta g_k \quad (k = 0, 1).\end{aligned}\tag{21}$$

We note for completeness, that one needs an additional counterterm in the action to cancel loop-induced contributions to the effective action which are linear in ϕ_R , i.e.

$$- \int_x \delta t_1 \phi_R(x).\tag{22}$$

At this stage, we can already give the renormalized equations of motions

$$[(1 + \delta Z_{\phi,2})\square_x + \widehat{m}_2^2(x)] \phi_R(x) = -\delta t_1 - \frac{(\alpha_R + \delta\alpha_1)}{2}G_R(x,x) - (g_R + \delta g_1)\text{tr}[D_R(x,x)],\tag{23}$$

$$[(1 + \delta Z_{\phi,0})\square_x + \widehat{m}_0^2(x)] G_R(x,y) = \delta_C(x-y) - \int_z \Pi(x,z)G_R(z,y),\tag{24}$$

$$[\text{i}(1 + \delta Z_{\psi,0})\not{\partial}_x - \widehat{M}_0(x)] D_R(x,y) = \delta_C(x-y) - \int_z \Sigma(x,z)D_R(z,y),\tag{25}$$

with

$$\widehat{m}_2^2(x) = m_R^2 + \delta m_2^2 + \frac{1}{2}(\alpha_R + \delta\alpha_3)\phi_R(x) + \frac{1}{6}(\lambda_R + \delta\lambda_4)\phi_R^2(x) + \frac{1}{2}(\lambda_R + \delta\lambda_2)G_R(x, x), \quad (26)$$

$$\widehat{m}_0^2(x) = m_R^2 + \delta m_0^2 + \frac{1}{4}(\lambda_R + \delta\lambda_0)G_R(x, x) + \frac{1}{2}(\alpha_R + \delta\alpha_3)\phi_R(x) + \frac{1}{4}(\lambda_R + \delta\lambda_2)\phi_R^2(x), \quad (27)$$

$$\widehat{M}_0(x) = (M_R + \delta M_0) + (g_R + \delta g_1)\phi_R(x), \quad (28)$$

$$\begin{aligned} \Pi(x, z) = & -\frac{i[(\alpha_R + \delta\alpha_0) + (\lambda_R + \delta\lambda_1)\phi_R(x)] [(\alpha_R + \delta\alpha_0) + (\lambda_R + \delta\lambda_1)\phi_R(z)]}{4} G_R^2(x, z) \\ & + \frac{i2(g_0 + \delta g_0)^2}{2} \text{tr}[D_R(x, z)D_R(z, x)], \end{aligned} \quad (29)$$

$$\Sigma(x, z) = \frac{i(g_R + \delta g_0)^2}{2} G_R(x, z) [D_R(x, z) + D_R(z, x)]. \quad (30)$$

Here, we have split the self-energies $\overline{\Pi}(x, z)$ and $\overline{\Sigma}(x, z)$ into non-local contributions $\Pi(x, z)$ and $\Sigma(x, z)$ and local ones which are absorbed in $\widehat{m}_0^2(x)$ and $\widehat{M}_0(x)$, respectively. Note that the integral on the right sides of (24) and (25) are the previously mentioned memory integrals.

One can solve (23)–(25) numerically for a given set of initial conditions. However, before one can start such a task, one must determine the yet unspecified counterterms. To this end, we use an on-shell scheme, detailed in the next section.

3 Renormalization: Generic Aspects

It is known that the Bogoliubov-Parasiuk-Hepp-Zimmermann (BPHZ) procedure [32–34], which is used in standard QFT to determine the structure of the divergences, does not suffice in the case of the 2PI formalism (see, for e.g., [31] and references therein). This is caused by the resummed nature of the 2-point functions G and D . The solution to this challenge is the auxiliary vertex functions which can be resummed such that a consistent renormalization with only a finite number of counterterms is possible.

The corresponding 2PI kernels, which enter the corresponding Bethe-Salpeter equations (BSE) are [28, 31]

$$\overline{\Lambda}^{(4)}(x_1, x_2, x_3, x_4) \equiv 4 \frac{\delta^2 \Gamma_{\text{int}}^{2\text{PI}}}{\delta G(x_1, x_2) \delta G(x_3, x_4)} \Big|_{\overline{\phi}, \overline{G}, \overline{D}}, \quad (31)$$

$$\Lambda_{\psi\psi}(x_1, x_2, x_3, x_4)_{(ab),(cd)} \equiv - \frac{\delta^2 \Gamma_{\text{int}}^{2\text{PI}}}{\delta D^{ba}(x_1, x_2) \delta D^{cd}(x_3, x_4)} \Big|_{\overline{\phi}, \overline{G}, \overline{D}}, \quad (32)$$

$$\Lambda_{\psi\phi}^{(4)}(x_1, x_2, x_3, x_4)_{ab} \equiv -2 \frac{\delta^2 \Gamma_{\text{int}}^{2\text{PI}}}{\delta D^{ba}(x_1, x_2) \delta G(x_3, x_4)} \Big|_{\bar{\phi}, \bar{G}, \bar{D}} \quad (33)$$

$$= \Lambda_{\phi\psi}^{(4)}(x_3, x_4, x_1, x_2)_{ab} \equiv -2 \frac{\delta^2 \Gamma_{\text{int}}^{2\text{PI}}}{\delta G(x_3, x_4) \delta D^{ab}(x_1, x_2)} \Big|_{\bar{\phi}, \bar{G}, \bar{D}}, \quad (34)$$

where we have denoted spinor indices through lowercase Latin alphabets. At this stage, we still need to take into account that a loop with four internal fermions can generate a divergent contribution to the quartic scalar coupling. This can be taken care of by introducing the following modified kernel for scalars

$$\begin{aligned} \tilde{\Lambda}_{\phi\phi}(x_1, x_2, x_3, x_4) &= \bar{\Lambda}^{(4)}(x_1, x_2, x_3, x_4) \\ &- i \int_{y_1 \dots y_4} \text{tr} \left[\bar{D}(y_1, y_3) \bar{\Lambda}_{\phi\psi}^{(4)}(x_1, x_2, y_1, y_2) \bar{D}(y_2, y_4) \bar{\Lambda}_{\psi\phi}(y_3, y_4, x_3, x_4) \right] \\ &+ i \int_{y_1 \dots y_8} \text{tr} \left[\bar{D}(y_1, y_3) \Lambda_{\phi\psi}^{(4)}(x_1, x_2, y_1, y_2) \bar{D}(y_2, y_4) V_{\psi\psi}(y_3, y_4, y_5, y_6) \right. \\ &\quad \left. \bar{D}(y_5, y_7) \Lambda_{\psi\phi}^{(4)}(y_7, y_8, x_3, x_4) \bar{D}(y_6, y_8) \right]. \end{aligned} \quad (35)$$

where the trace in the second line (“tr”) is over the spinor indices. Now, we are in the position to define the vertex functions which are given by the following Bethe-Salpeter equations

$$\begin{aligned} \bar{V}^{(4)}(x_1, x_2, x_3, x_4) &= \tilde{\Lambda}_{\phi\phi}(x_1, x_2, x_3, x_4) \\ &+ \frac{i}{2} \int_{y_1 \dots y_4} \tilde{\Lambda}_{\phi\phi}(x_1, x_2, y_1, y_2) \bar{G}(y_1, y_3) \bar{G}(y_2, y_4) \bar{V}^{(4)}(y_3, y_4, x_3, x_4), \end{aligned} \quad (36)$$

$$\begin{aligned} V_{\psi\psi}(x_1, x_2, x_3, x_4)_{ab,cd} &= \Lambda_{\psi\psi}(x_1, x_2, x_3, x_4)_{ab,cd} \\ &+ i \int_{y_1 \dots y_4} \Lambda_{\psi\psi}(x_1, x_2, y_1, y_2)_{ab,ef} \bar{D}(y_1, y_3)_{eg} \\ &\quad V_{\psi\psi}(y_3, y_4, x_3, x_4)_{ef,cd} \bar{D}(y_2, y_4)_{fb}, \end{aligned} \quad (37)$$

$$\begin{aligned} V_{\psi\phi}^{(4)}(x_1, x_2, x_3, x_4)_{ab} &= \Lambda_{\psi\phi}^{(4)}(x_1, x_2, x_3, x_4)_{ab} \\ &+ i \int_{y_1 \dots y_4} \Lambda_{\psi\phi}^{(4)}(x_1, x_2, y_1, y_2)_{ae} \bar{D}(y_1, y_3)_{ef} \\ &\quad V_{\psi\phi}^{(4)}(y_3, y_4, x_3, x_4)_{fb} \bar{G}(y_2, y_4). \end{aligned} \quad (38)$$

In the study of the vacuum structure of a theory, it is useful to consider any ϕ and evaluate the corresponding two-point function (Green’s function) $G(\phi)$. This leads to a 2PI effective action $\Gamma[\phi] = \Gamma_{2\text{PI}}[\phi, G(\phi)]$ which gives rise to a 2PI improved effective potential. When studying phase transitions in the 2PI formalism, this is the object to consider when looking for the vacuum states of the theory. The two-point functions in this case can be evaluated from the stationarity condition (12), leading to the gap equation for the scalar

propagator

$$\overline{G}^{-1}(x, y; \phi) = G_0^{-1}(x, y; \phi) - \overline{\Pi}(x, y; \phi) \quad (39)$$

and similarly one for the fermionic propagator

$$\overline{D}^{-1}(x, y; \phi) = D_0^{-1}(x, y; \phi) - \overline{\Sigma}(x, y; \phi). \quad (40)$$

From this perspective, the stationarity condition for the scalar field becomes

$$\Gamma^{(1)}(x) \equiv \left. \frac{\delta \Gamma^{2\text{PI}}}{\delta \phi(x)} \right|_{\overline{\phi}, \overline{G}, \overline{D}} \stackrel{!}{=} 0 \quad (41)$$

$$= \left. \frac{\delta \Gamma^{2\text{PI}}}{\delta \phi(x)} \right|_{\overline{\phi}, \overline{G}, \overline{D}} + \int_{y_1, y_2} \left. \frac{\delta \Gamma^{2\text{PI}}}{\delta G(y_1, y_2)} \right|_{\overline{\phi}, \overline{G}, \overline{D}} \frac{\delta G(y_1, y_2)}{\delta \phi(x)} + \int_{y_1, y_2} \text{tr} \left\{ \left. \frac{\delta \Gamma^{2\text{PI}}}{\delta D(y_1, y_2)} \right|_{\overline{\phi}, \overline{G}, \overline{D}} \frac{\delta D(y_1, y_2)}{\delta \phi(x)} \right\} \quad (42)$$

where $\Gamma^{(1)}$ denotes the physical one-point function. The second and third terms of the last line vanish due to the stationarity conditions.

Moreover, we will require the n -point functions

$$\Gamma^{(n)}(x_1, \dots, x_n) = \left. \frac{\delta^n \Gamma^{2\text{PI}}}{\delta \phi(x_1) \dots \delta \phi(x_n)} \right|_{\overline{\phi}, \overline{G}, \overline{D}}. \quad (43)$$

These are related to the derivatives of the 2PI generating functional $\Gamma^{2\text{PI}}$. However, one has to take care since the two-point function obtained from (39) depends on ϕ and thus the chain rule must be used. As a consequence, a system of coupled integral equations emerges. In general, these equations have the following form

$$\begin{aligned} \frac{\delta^n i\Gamma}{\delta \phi(x_1) \dots \delta \phi(x_n)} &= \mathcal{A}^{(n)}(x_1, \dots, x_n) \\ &+ \int_{z_1 \dots z_4} \left. \frac{\delta^2 i\Gamma_{\text{int}}^{2\text{PI}}}{\delta \phi(x_1) G(z_1, z_2)} \right|_{\overline{\phi}, \overline{G}, \overline{D}} \overline{G}(z_1, z_3) \frac{\delta^{n-1} \overline{\Pi}(z_3, z_4)}{\delta \phi(x_2) \dots \delta \phi(x_n)} \overline{G}(z_4, z_2) \\ &+ \int_{z_1 \dots z_4} \text{tr} \left\{ \left. \frac{\delta^2 \Gamma_{\text{int}}^{2\text{PI}}}{\delta \phi(x_1) \delta D(z_1, z_2)} \right|_{\overline{\phi}, \overline{G}, \overline{D}} \overline{D}(z_1, z_3) \frac{\delta^{n-1} \overline{\Sigma}(z_3, z_4)}{\delta \phi(x_2) \dots \delta \phi(x_n)} \overline{D}(z_4, z_2) \right\} \end{aligned} \quad (44)$$

$$\begin{aligned} \frac{\delta^n \overline{\Pi}(y_1, y_2)}{\delta \phi(x_1) \dots \delta \phi(x_n)} &= \mathcal{B}^{(n)}(y_1, y_2, x_1, \dots, x_n) \\ &+ \int_{z_1 \dots z_4} \left. \frac{\delta^2 2i\Gamma_{\text{int}}^{2\text{PI}}}{\delta G(y_1, y_2) \delta G(z_1, z_2)} \right|_{\overline{\phi}, \overline{G}, \overline{D}} \overline{G}(z_1, z_3) \frac{\delta^{n-1} \overline{\Pi}(z_3, z_4)}{\delta \phi(x_1) \dots \delta \phi(x_n)} \overline{G}(z_4, z_2) \\ &+ \int_{z_1 \dots z_4} \text{tr} \left\{ \left. \frac{\delta^2 2i\Gamma_{\text{int}}^{2\text{PI}}}{\delta G(y_1, y_2) \delta D(z_1, z_2)} \right|_{\overline{\phi}, \overline{G}, \overline{D}} \overline{D}(z_1, z_3) \frac{\delta^{n-1} \overline{\Sigma}(z_3, z_4)}{\delta \phi(x_1) \dots \delta \phi(x_n)} \overline{D}(z_4, z_2) \right\} \end{aligned} \quad (45)$$

$$\begin{aligned}
\frac{\delta^n \bar{\Sigma}(y_1, y_2)}{\delta\phi(x_1) \dots \delta\phi(x_n)} &= \mathcal{C}^{(n)}(y_1, y_2, x_1, \dots, x_n) \\
&+ \int_{z_1 \dots z_4} \frac{\delta^2 \Gamma_{\text{int}}^{2\text{PI}}}{\delta D(y_1, y_2) \delta G(z_1, z_2)} \Big|_{\bar{\phi}, \bar{G}, \bar{D}} \bar{G}(z_1, z_3) \frac{\delta^{n-1} \bar{\Pi}(z_3, z_4)}{\delta\phi(x_1) \dots \delta\phi(x_n)} \bar{G}(z_4, z_2) \\
&+ \int_{z_1 \dots z_4} \frac{\delta^2 \Gamma_{\text{int}}^{2\text{PI}}}{\delta D(y_1, y_2) \delta D(z_1, z_2)} \Big|_{\bar{\phi}, \bar{G}, \bar{D}} \bar{D}(z_1, z_3) \frac{\delta^{n-1} \bar{\Sigma}(z_3, z_4)}{\delta\phi(x_1) \dots \delta\phi(x_n)} \bar{D}(z_4, z_2)
\end{aligned} \tag{46}$$

The functions $\mathcal{A}^{(n)}$, $\mathcal{B}^{(n)}$ and $\mathcal{C}^{(n)}$ contain both various derivatives of $\Gamma_{\text{int}}^{2\text{PI}}$ with respect to ϕ , G and D at the stationarity point $(\bar{\phi}, \bar{G}, \bar{D})$ [31]. Moreover, they contain lower derivatives $\delta^k \bar{\Pi} / \delta\phi^k$ and $\delta^k \bar{\Sigma} / \delta\phi^k$ ($k = 1, \dots, n-1$). Consequently, n -point functions are expressed solely via parts of the 2PI generating functional and their derivatives. This comes at the expense of infinite resummations of self-energy diagrams and their derivatives. A formal solution to the self-energy equations can be given in terms of the various vertex functions. Using these, the solutions to (45) and (46) are given by

$$\begin{aligned}
\frac{\delta^n \bar{\Pi}(y_1, y_2)}{\delta\phi(x_1) \dots \delta\phi(x_n)} &= \mathcal{B}^{(n)}(y_1, y_2, x_1, \dots, x_n) \\
&+ \frac{i}{2} \int_{z_1 \dots z_4} \bar{V}^{(4)}(x_1, x_2, z_1, z_2) \bar{G}(z_1, z_3) \mathcal{B}^{(n)}(z_3, z_4, x_1, \dots, x_n) \bar{G}(z_4, z_2) \\
&+ i \int_{z_1 \dots z_4} \text{tr} \left\{ V_{\phi\psi}^{(4)}(x_1, x_2, z_1, z_2) \bar{D}(z_1, z_3) \mathcal{C}^{(n)}(z_3, z_4, x_1, \dots, x_n) \bar{D}(z_4, z_2) \right\}.
\end{aligned} \tag{47}$$

$$\begin{aligned}
\frac{\delta^n \bar{\Sigma}(y_1, y_2)}{\delta\phi(x_1) \dots \delta\phi(x_n)} &= \mathcal{C}^{(n)}(y_1, y_2, x_1, \dots, x_n) \\
&+ i \int_{z_1 \dots z_4} V_{\psi\phi}^{(4)}(x_1, x_2, z_1, z_2) \mathcal{B}^{(n)}(z_3, z_4, x_1, \dots, x_n) \bar{G}(z_1, z_3) \bar{G}(z_4, z_2) \\
&+ i \int_{z_1 \dots z_4} V_{\psi\psi}^{(4)}(x_1, x_2, z_1, z_2) \bar{D}(z_1, z_3) \mathcal{C}^{(n)}(z_3, z_4, x_1, \dots, x_n) \bar{D}(z_4, z_2).
\end{aligned} \tag{48}$$

From these equations, one can then obtain solutions to (44). In addition, we would require an auxiliary scalar vertex function

$$\begin{aligned}
V^{(4)}(x_1, x_2, x_3, x_4) &= \Lambda^{(4)}(x_1, x_2, x_3, x_4) \\
&+ \frac{i}{2} \int_{y_1 \dots y_4} \Lambda^{(4)}(x_1, x_2, y_1, y_2) \bar{G}(y_1, y_3) \bar{G}(y_2, y_4) \bar{V}^{(4)}(y_3, y_4, x_3, x_4),
\end{aligned} \tag{49}$$

with

$$\Lambda^{(4)}(x_1, x_2, x_3, x_4) \equiv 2 \frac{\delta^3 \Gamma_{\text{int}}^{2\text{PI}}}{\delta G(x_1, x_2) \delta\phi(x_3) \delta\phi(x_4)} \Big|_{\bar{\phi}, \bar{G}, \bar{D}}. \tag{50}$$

It was mentioned in the previous section that actual calculations require an approximation of the 2PI generating functional. In terms of renormalizability, there are certain requirements to be met when choosing the diagrams for $\Gamma_{\text{int}}^{2\text{PI}}$, which becomes apparent when using the BPHZ analysis for the identification of necessary subtractions. Therein, all diagrams are examined for possible sub-divergences, by employing Weinberg's theorem [35]. Whenever a part of a diagram is potentially divergent, this part is shrunk to an effective vertex. The new topology created this way must be part of the renormalized $\Gamma_{\text{int}}^{2\text{PI}}$, with the effective vertex replaced by counterterms in order to cancel divergences.

Effectively, this means that we are dealing with a truncation in perturbation theory where some parts have been resummed, implying that one has to take different mass and coupling constant counterterms, depending on the combination of one- and two-point functions connecting to a 'vertex'. According to [31], renormalization may be carried out in the vacuum at temperature $T = 0$. It is most convenient to work in momentum space, which allows us to employ the usual techniques to determine the various counterterms in an on-shell scheme. We extend the usual on-shell conditions of standard QFT, see for e.g. [36], to the 2PI formalism as follows

$$Z_{\phi,0} G_R^{-1}(p) \Big|_{p^2=m_R^2} = Z_{\phi,2} \Gamma_{\phi}^{(2)}(p) \Big|_{p^2=m_R^2} = 0, \quad (51)$$

$$Z_{\phi,0} \frac{\partial}{\partial p^2} G_R^{-1}(p) \Big|_{p^2=m_R^2} = Z_{\phi,2} \frac{\partial}{\partial p^2} \Gamma_{\phi}^{(2)}(p) \Big|_{p^2=m_R^2} = 1, \quad (52)$$

$$Z_{\psi,0} D_R^{-1}(p) u(p) \Big|_{p^2=M_R^2} = 0, \quad \lim_{p^2 \rightarrow M_R^2} Z_{\psi,0}^{-1} \left(\frac{\not{p} + M_R}{p^2 - M_R^2} \right) D_R^{-1}(p) u(p) = u(p), \quad (53)$$

$$\begin{aligned} Z_{\phi,0}^2 \bar{V}^{(4)}(p_1, p_2, p_3, p_4) \Big|_{p_i^2=m_R^2} &= Z_{\phi,2} Z_{\phi,0} V^{(4)}(p_1, p_2, p_3, p_4) \Big|_{p_i^2=m_R^2} \\ &= Z_{\phi,2}^2 \Gamma^{(4)}(p_1, p_2, p_3, p_4) \Big|_{p_i^2=m_R^2} = -\lambda_R, \end{aligned} \quad (54)$$

$$Z_{\phi,0} Z_{\phi,2}^{\frac{1}{2}} V^{(3)}(p_1, p_2, p_3) \Big|_{p_2^2=p_3^2=m_R^2} = Z_{\phi,2}^{\frac{3}{2}} \Gamma^{(3)}(p_1, p_2, p_3) \Big|_{p_2^2=p_3^2=m_R^2} = -\alpha_R, \quad (55)$$

$$Z_{\psi,2} Z_{\phi,2}^{\frac{1}{2}} \bar{u}(p_1) V_{\psi\phi}^{(3)}(p_1, p_2, p_3) u(p_2) \Big|_{p_2^2=M_R^2, p_3^2=m_R^2} = -g_R \quad (56)$$

where $u(p)$ is an on-shell spinor and $\bar{u}(p)$ is its Dirac conjugate. $V^{(3)}$ and $V_{\psi\phi}^{(3)}$ denote pure scalar and fermion-fermion-scalar three-point vertices respectively, that will be discussed in the relevant section. Note that we use the same symbols to denote the n -point functions in configuration and momentum space indicated only by the arguments. The momentum arguments are not independent, but related via momentum conservation, for e.g. $p_1 + p_2 = p_3 + p_4$ for the four-point functions and $p_1 = p_2 + p_3$ for the three-point functions.

Note that we have made a choice to implement the same renormalization conditions for the physical two-point functions of the fields and the propagators, as in [23, 25]. We do the same for the physical n -point functions of the scalar fields, and the corresponding vertex functions. One may also choose to renormalize these functions to different coupling constants, such as in [37], but these correspond to shifts in the various counterterms.

4 Renormalization with only Scalars

We begin with scalars, which can be considered to be a limit where the fermions are so heavy that they need to be integrated out. This allows us to detail the intricacies of the renormalization procedure, without the complication of additional Lorentz structures. As a novel aspect, we present here not only the counterterms for the symmetric phase, but also in the broken one.

4.1 Revisiting the Hartree Approximation

This case has been treated in literature already several times [17, 18, 25] and is summarized here to exemplify some of the details involved. Moreover, we have obtained new results, which to our knowledge have not been presented in literature so far, such as finite contributions to the wave function renormalization.

In this approximation, one sets $\alpha = g = 0$ and takes only the leading contribution to Γ_2 into account. Expressing $\Gamma_{\text{int}}^{2\text{PI}}$ in terms of renormalized quantities, we get

$$\begin{aligned} \Gamma_{\text{int}}^{2\text{PI}}[\phi_R, G_R] = & -\frac{1}{2} \int_x (\delta Z_{\phi,0} \square_x + \delta m_0^2) G_R(x, y) \Big|_{x=y} - \frac{1}{2} \int_x \phi_R(x) (\delta Z_{\phi,2} \square_x + \delta m_2^2) \phi_R(x) \\ & - \int_x \left[\frac{1}{8} (\lambda_R + \delta\lambda_0) G_R^2(x, x) + \frac{1}{4} (\lambda_R + \delta\lambda_2) G_R(x, x) \phi_R^2(x) + \frac{1}{4!} (\lambda_R + \delta\lambda_4) \phi_R^4(x) \right]. \end{aligned} \quad (57)$$

This gives the four-point kernel

$$\bar{\Lambda}^{(4)} = 4 \frac{\delta^2 \Gamma_{\text{int}}^{2\text{PI}}}{\delta G_R(k) \delta G_R(q)} = -(\lambda_R + \delta\lambda_0), \quad (58)$$

which is evidently independent of the (external) momentum. Thus, the BSE (36) simplifies considerably within the Hartree approximation. As the vertex function is an infinite resummation of iterations of this kernel, stitched together by loops with two propagators (see Fig. 1), the only origin of a momentum dependence in $\bar{V}^{(4)}$ is from the loop function depending on the sum of external momenta $p = p_1 + p_2$. For brevity, we will thus use the notation $\bar{V}^{(4)}(p) \equiv \bar{V}^{(4)}(p_1, p_2, p_3, p_4)$ throughout this section. Accordingly, the BSE is expressed as

$$\bar{V}^{(4)}(p) = -(\lambda_R + \delta\lambda_0) - \frac{i}{2} (\lambda_R + \delta\lambda_0) \bar{V}^{(4)}(p) \int_q G_R(q) G_R(p+q). \quad (59)$$

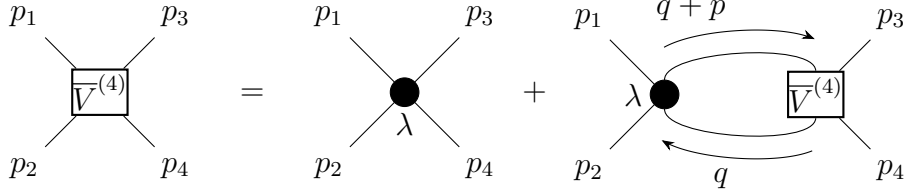


Figure 1: Illustration of the BSE in the Hartree approximation. Here, the convention is $p_{1,2}$ are incoming four-momenta and $p_{3,4}$ are outgoing, with $p = p_1 + p_2$.

At this point, it is convenient to calculate p^2 in the center of mass (COM) system. This gives the familiar result

$$p^2 = (p_1 + p_2)^2 = 4E_*^2, \quad (60)$$

where $2E_*$ is the COM energy. Let $p_*^2 = 4m_R^2$ be the renormalization point corresponding to the COM three-momentum $|\vec{p}_*| = 0$ and let

$$\bar{V}^{(4)}(p_*) = -\lambda_R. \quad (61)$$

This allows us to solve exactly for the counterterm

$$\delta\lambda_0 = -\lambda_R + \frac{\lambda_R}{1 - \frac{1}{2}\lambda_R\mathcal{I}(p_*^2)} \quad \text{with} \quad \mathcal{I}(p^2) = i \int_q G_R(q)G_R(p+q), \quad (62)$$

which we can insert in (59) to obtain the vertex function

$$\bar{V}^{(4)}(p) = -\frac{\lambda_R}{1 - \frac{\lambda_R}{2}(\mathcal{I}(p_*^2) - \mathcal{I}(p^2))}. \quad (63)$$

From this, we can immediately observe that $\bar{V}^{(4)}(p)$ is finite as any potential divergences present in the loop integral $\mathcal{I}(p^2)$ cancels in the difference $\mathcal{I}(p_*^2) - \mathcal{I}(p^2)$. Furthermore, the renormalization of the auxiliary vertex $V(p)$ proceeds along similar lines as

$$\Lambda^{(4)} = 2 \frac{\delta^3 \Gamma_{\text{int}}^{2\text{PI}}}{\delta^2 \phi_R \delta G_R(q)} = -(\lambda_R + \delta\lambda_2). \quad (64)$$

Using this in (36) and the result (63), along with the renormalization condition (61), we obtain

$$\delta\lambda_2 = \delta\lambda_0 \quad \text{and} \quad V^{(4)}(p) = \bar{V}^{(4)}(p). \quad (65)$$

We have made a choice to implement the same renormalization conditions for both vertex functions. We will later do the same for the propagator and the two-point function of the scalar field, as in [23, 25], as well for the physical n -point functions of the scalar fields corresponding to the vertex functions. One may also choose to renormalise these functions to

different parameters, such as in [37], but these correspond to shifts in the various counterterms.

The determination of these counterterms via the BSEs allows us to treat the subdivergences, which are not accounted for by the usual BHPZ procedure, that would appear in the renormalization of the two-point function [18, 31], for which we now turn to the gap equation

$$\begin{aligned} iG_R^{-1}(p) &= (p^2 - m_R^2) - i\bar{\Pi}(p^2) \\ &= (p^2 - m_R^2) + (\delta Z_{\phi,0} p^2 - \delta m_0^2) - \frac{(\lambda_R + \delta\lambda_2)}{2} \phi_R^2 - \frac{(\lambda_R + \delta\lambda_0)}{2} \int_q G_R(q), \end{aligned} \quad (66)$$

where p here is the external momentum. Having determined $\delta\lambda_0$ and $\delta\lambda_2$, we seek for the counterterms $\delta Z_{\phi,0}$ and δm_0^2 which can be used to treat the divergences that can be accounted for by the BHPZ procedure. Enforcing the on-shell renormalization conditions (51), we have

$$iG_R^{-1}(p) \Big|_{p^2=m_R^2} = -i\bar{\Pi}(p^2) \Big|_{p^2=m_R^2} \stackrel{!}{=} 0, \quad (67)$$

$$i \frac{\partial}{\partial p^2} G_R^{-1}(p) \Big|_{p^2=m_R^2} = 1 - i \frac{\partial}{\partial p^2} \bar{\Pi}(p^2) \Big|_{p^2=m_R^2} \stackrel{!}{=} 1. \quad (68)$$

From (68), we have

$$\delta Z_{\phi,0} = 0 \quad (69)$$

and then (67) gives

$$\delta m_0^2 = -\frac{\lambda_R + \delta\lambda_2}{2} \phi_R^2 - \frac{\lambda_R + \delta\lambda_0}{2} \int_q G_R(q). \quad (70)$$

If we substitute this back into (66), we obtain

$$iG_R^{-1}(p^2) = p^2 - m_R^2, \quad (71)$$

or, in other words, the full propagator is identically the bare one. Consequently, all integrals over propagators can be expressed in terms of the well-known Passarino-Veltman functions [36]

$$\int_q G_R(q) = \frac{1}{16\pi^2} A_0(m_R^2) \quad (72)$$

$$\mathcal{I}(p) \equiv i \int_q G_R(q) G_R(p+q) = \frac{1}{16\pi^2} B_0(p^2, m_R^2, m_R^2), \quad (73)$$

For the counterterms, we thus find

$$\delta\lambda_0 = -\lambda_R - 32\pi^2\epsilon + \mathcal{O}(\epsilon^2) = \delta\lambda_2, \quad (74)$$

$$\delta Z_0 = 0 + \mathcal{O}(\epsilon), \quad \text{and} \quad \delta m_0^2 = -m_R^2 + \mathcal{O}(\epsilon), \quad (75)$$

$$i\Gamma_{\text{int}}^{2\text{PI}} = \bullet \qquad G_R(x_1, x_2) = 1 \text{ --- } 2$$

$$\frac{i\delta^2\Gamma_{\text{int}}^{2\text{PI}}}{\delta\phi_R(x_1)\delta\phi_R(x_2)} = i\Pi(x_1, x_2) = 1 \circ \bullet \text{ --- } \circ 2 \qquad i\bar{\Pi}(x_1, x_2) = \frac{1}{2} \begin{array}{|c|} \hline \square \blacksquare \\ \hline \end{array}$$

$$i\bar{V}^{(4)}(x_1, x_2, x_3, x_4) = \frac{1}{2} \begin{array}{|c|} \hline \square \begin{array}{|c|} \hline i\bar{V}^{(4)} \\ \hline \end{array} \square \\ \hline \end{array} \begin{array}{l} 3 \\ 4 \end{array} \qquad \frac{i\delta\bar{\Pi}(x_1, x_2)}{\delta\phi_R(x_3)} = \frac{1}{2} \begin{array}{|c|} \hline \blacksquare \\ \hline \end{array} \text{ --- } \circ 3$$

Figure 2: Graphical representation of basic building blocks

and also the expression for the vertex function,

$$\bar{V}^{(4)}(p) = -\frac{\lambda_R}{1 - \frac{\lambda_R}{32\pi^2} [B_0(4m_R^2, m_R^2, m_R^2) - B_0(p^2, m_R^2, m_R^2)]}. \quad (76)$$

We mention, for completeness, that we did not assume $\phi_R = 0$, i.e. these relations hold true in the unbroken and broken phases. Furthermore, in the unbroken phase we can exploit the \mathbb{Z}_2 symmetry of the Hartree approximation and make use of the identity [31]

$$\left. \frac{\delta^2\Gamma_{\text{int}}^{2\text{PI}}}{\delta\phi_R^2} \right|_{\phi_R=0} + (\delta Z_2 p^2 - \delta m_2^2) = 2 \left. \frac{\delta\Gamma_{\text{int}}^{2\text{PI}}}{\delta G_R} \right|_{\phi_R=0} + (\delta Z_0 p^2 - \delta m_0^2) \quad (77)$$

to relate the counterterms for the propagator and the field. Due to the fact that we have imposed the same renormalization conditions for $\Gamma^{(2)}$ and G_R^{-1} (c.f. (51)), we find

$$\delta Z_{\phi,2} = \delta Z_{\phi,0} \quad \text{and} \quad \delta m_0^2 = \delta m_2^2. \quad (78)$$

We now demonstrate explicitly that these relations do not hold for $\phi_R \neq 0$. It is useful at this point to introduce a diagrammatic representation of the various integral equations that we will encounter, which is based on the one in [31]. The basic building blocks are given in Fig. 2.

We first examine the physical two-point function, for which we have the following integral equation

$$\begin{aligned} \Gamma^{(2)}(x_1, x_2) &\equiv \frac{\delta^2\Gamma^{2\text{PI}}}{\delta\phi_R(x_1)\delta\phi_R(x_2)} \\ &= iG_{0,R}^{-1}(x_1, x_2) + \left. \frac{\delta^2\Gamma_{\text{int}}^{2\text{PI}}}{\delta\phi_R(x_1)\delta\phi_R(x_2)} \right|_{G_R} \\ &+ \int_{y_1, y_2, y_3, y_4} \left. \frac{\delta^2\Gamma_{\text{int}}^{2\text{PI}}}{\delta\phi_R(x_1)\delta G_R(y_1, y_2)} \right|_{G_R} G_R(y_1, y_3) \frac{\delta\bar{\Pi}_R(y_3, y_4)}{\delta\phi_R(x_2)} G_R(y_4, y_2). \end{aligned} \quad (79)$$

Using the elements presented in Fig. 2, this equation reads in graphical form

$$\frac{\delta^2 \Gamma^{2PI}}{\delta\phi_R(x_1)\delta\phi_R(x_2)} = iG_{0,R}^{-1}(x_1, x_2) + 1 \circ \text{---} \bullet \text{---} \circ 2 + \frac{1}{2} 1 \circ \text{---} \bullet \text{---} \square \text{---} \circ 2 \quad (80)$$

We can replace the derivative of the self-energy w.r.t. a field expectation value $\delta\bar{\Pi}/\delta\phi_R$ using the following graphical representation (c.f. (47))

$$\frac{1}{2} \square \text{---} \circ 3 = \frac{1}{2} \square \text{---} \bullet \text{---} \circ 3 + \frac{1}{2} \frac{1}{2} \square \text{---} \overline{V}^{(4)} \text{---} \bullet \text{---} \circ 3 \quad (81)$$

Inserting this into the integral equation (80), we obtain in momentum space

$$\begin{aligned} \Gamma^{(2)}(p) &= (p^2 - m_R^2) + (\delta Z_{\phi,2} p^2 - \delta m_2^2) - \frac{1}{2}(\lambda_R + \delta\lambda_4)\phi_R^2 - \frac{1}{2}(\lambda_R + \delta\lambda_2) \int_q G_R(q) \\ &\quad - \frac{1}{8}(\lambda_R + \delta\lambda_2)^2 [\mathcal{I}(p^2)] \phi_R^2 + \frac{1}{16}(\lambda_R + \delta\lambda_2)^2 [\mathcal{I}(p^2)]^2 \overline{V}^{(4)}(p) \phi_R^2 \\ &= [(1 + \delta Z_{\phi,2})p^2 - 2m_R^2 - \delta m_2^2] - \frac{1}{2}(\lambda_R + \delta\lambda_4)\phi_R^2 \\ &\quad + \frac{\lambda_R \phi_R^2}{4} \left\{ 1 - \frac{\lambda_R}{32\pi^2} [B_0(p_*^2, m_R^2, m_R^2) - B_0(p^2, m_R^2, m_R^2)] \right\}^{-1} + O(\epsilon). \end{aligned} \quad (82)$$

Imposing the same renormalization conditions as for G_R , (51), this yields

$$\delta Z_{\phi,2} = \frac{\lambda_R^2 \phi_R^2}{128\pi^2} \dot{B}_0(m_R^2, m_R^2, m_R^2) \left\{ 1 - \frac{\lambda_R}{32\pi^2} [B_0(p_*^2, m_R^2, m_R^2) - B_0(m_R^2, m_R^2, m_R^2)] \right\}^{-1} \quad (83)$$

$$\begin{aligned} \delta m_2^2 &= -m_R^2 + m_R^2 \delta Z_{\phi,2} - \frac{(\lambda_R + \delta\lambda_4)\phi_R^2}{2} \\ &\quad + \frac{\lambda_R \phi_R^2}{4} \left\{ 1 - \frac{\lambda_R}{32\pi^2} [B_0(p_*^2, m_R^2, m_R^2) - B_0(m_R^2, m_R^2, m_R^2)] \right\}^{-1}, \end{aligned} \quad (84)$$

where

$$\dot{B}_0(p^2, m_R^2, m_R^2) = \left. \frac{\partial B_0(q^2, m_R^2, m_R^2)}{\partial q^2} \right|_{q^2=p^2}.$$

One recovers the equality with the corresponding counterterms for G_R in (78) when $\phi_R = 0$, as claimed in [31].

Finally, one needs to determine $\delta\lambda_4$. The treatment of the physical four-point function proceeds in the same manner as for the two-point function, but now a lot more diagrams contribute. An easy way to obtain the four-point function is to take the diagrammatical expression of the two-point function and then take two more derivatives with respect to the field ϕ_R . Application of the chain rule due to the ϕ_R dependence of G_R generates a variety of topologies. Here, we will first give the overview over all the topologies that contribute,

in order to generalise to additional couplings, and perform truncations appropriate to the Hartree approximation. For the sake of brevity, the four “legs” representing the external space-time points, previously denoted in the diagrams with numerical indices, are now suppressed and it is understood that all permutations of x_2, x_3 and x_4 contribute, as long as the resulting diagrams are not equivalent. An example of a diagram, where permutations must be considered, is

$$\begin{array}{c} \circ \\ | \\ \bullet \\ | \\ \circ \end{array} = \begin{array}{c} 4 \\ \circ \\ | \\ \bullet \\ | \\ \circ \end{array} + \begin{array}{c} 4 \\ \circ \\ | \\ \bullet \\ | \\ \circ \end{array} + \begin{array}{c} 3 \\ \circ \\ | \\ \bullet \\ | \\ \circ \end{array} \quad (85)$$

It is important to note that the index 1 is not part of the permutation. This happens because the diagrams are obtained by a subsequent differentiation with respect to the four fields $\phi_R(x_1), \dots, \phi_R(x_4)$. The first self-energy box only appears in the second differentiation and thus the 1-index is always attached to the $\Gamma_{\text{int}}^{2\text{PI}}$ blob. In the subsequent discussion, the leg to the left side is always considered to correspond to the 1-index. At first glance, this might seem to not be in line with the symmetry properties of the 4-point function, such as $\Gamma^{(4)}(x_1, x_2, x_3, x_4) = \Gamma^{(4)}(x_2, x_1, x_3, x_4)$ and so on. However, these properties are only hidden in the above case and are apparent once the identities of the self-energy boxes are inserted.

The diagrams that in principal contribute to the 4-point function are

$$\Gamma^{(4)} \equiv \frac{\delta^4 \Gamma}{\delta \phi^4} = \begin{array}{c} \circ \\ | \\ \bullet \\ | \\ \circ \end{array} + \frac{1}{2} \begin{array}{c} \circ \\ | \\ \bullet \\ | \\ \circ \end{array} + \frac{1}{4} \begin{array}{c} \circ \\ | \\ \bullet \\ | \\ \circ \end{array} + \frac{1}{8} \begin{array}{c} \circ \\ | \\ \bullet \\ | \\ \circ \end{array} + \begin{array}{c} \circ \\ | \\ \bullet \\ | \\ \circ \end{array} + \frac{1}{2} \begin{array}{c} \circ \\ | \\ \bullet \\ | \\ \circ \end{array} + \begin{array}{c} \circ \\ | \\ \bullet \\ | \\ \circ \end{array}$$

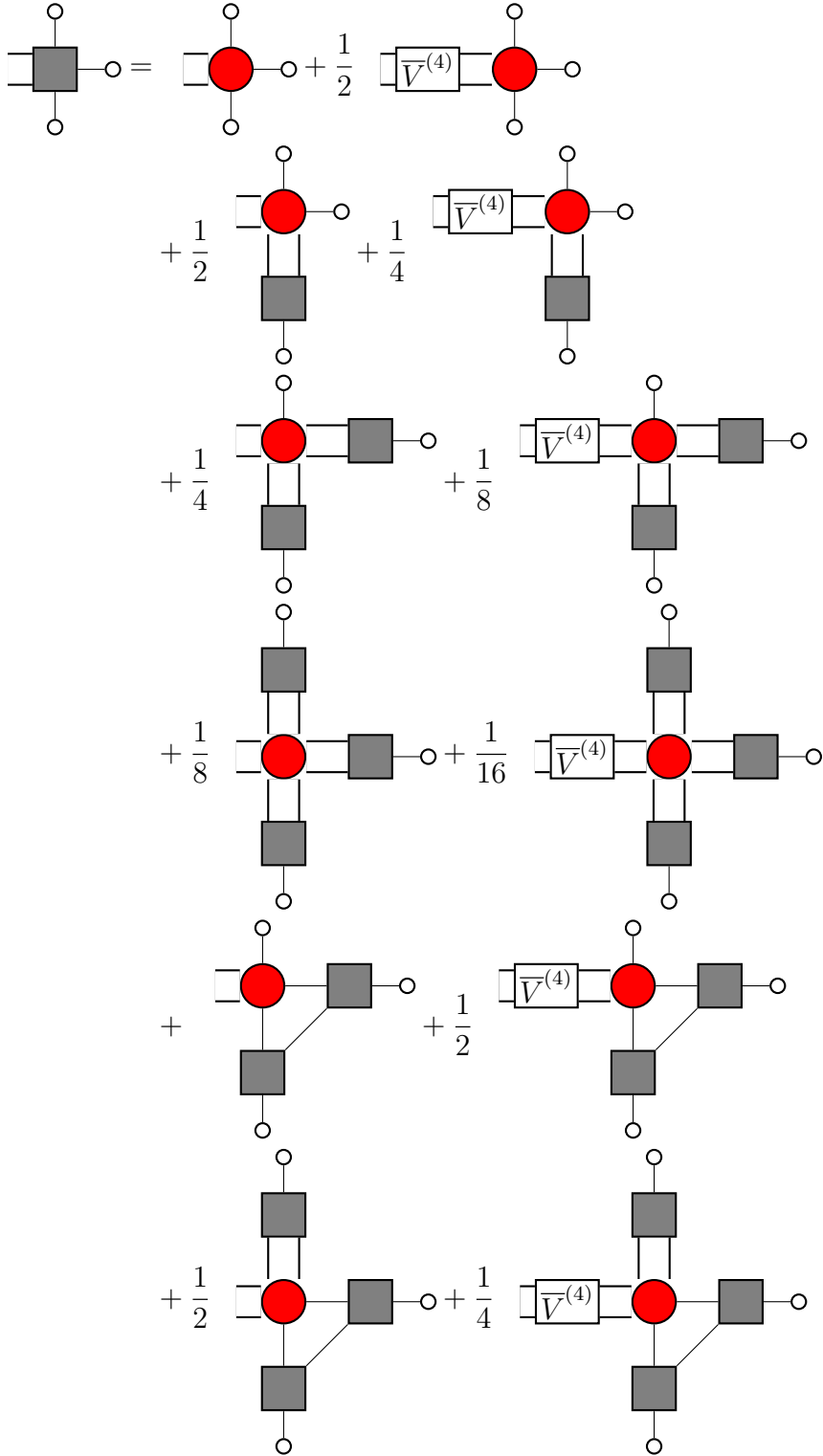
$$\begin{aligned}
& + \frac{1}{2} \text{diagram} + \frac{1}{4} \text{diagram} + \text{diagram} \\
& + \frac{1}{2} \text{diagram} .
\end{aligned} \tag{86}$$

The diagrams, where the $\Gamma_{\text{int}}^{2\text{PI}}$ blob is marked in red, do not contribute in the Hartree approximation due to the limited number of terms contained in $\Gamma_{\text{int}}^{2\text{PI}}$. This reduces the number of diagrams one has to consider by about half but this only works for the 2PI kernels and not for the self-energy boxes which adhere to their own integral equations. We have seen that derivatives of the self-energy with respect to one, two and three fields ϕ_R are present. The single derivative is given in (81). The other two can be expressed using diagrams that contain only the first derivative of the self-energy. We will continue to mark $\Gamma_{\text{int}}^{2\text{PI}}$ in red if the contribution vanishes in the Hartree approximation, and permutations of field indices are implied wherever they lead to non-equivalent topologies.

$$\begin{aligned}
& \text{diagram} = \text{diagram} + \frac{1}{2} \text{diagram} \\
& + \frac{1}{2} \text{diagram} + \frac{1}{4} \text{diagram} \\
& + \frac{1}{4} \text{diagram} + \frac{1}{8} \text{diagram} \\
& + \text{diagram} + \frac{1}{2} \text{diagram}
\end{aligned} \tag{87}$$

For the triple derivative $d^3\bar{\Pi}/d\phi_R^3$, it is more convenient to not insert instances of the double derivative $d^3\bar{\Pi}/d\phi_R^2$ as the expressions get too lengthy otherwise. One simply needs to substitute the corresponding diagrams from (87) at places where boxes with two field derivatives

appear. One then finds



The diagram shows a series of Feynman diagrams arranged in four rows, each representing a different topology. The diagrams are connected by plus signs and numerical coefficients. The vertices are represented by squares (grey or black) and circles (red or black). External lines are represented by circles. The diagrams are as follows:

- Row 1: A diagram with a central black circle vertex connected to four grey square vertices, which are further connected to external lines. Coefficient: $1/2$.
- Row 2: A diagram with a central red circle vertex connected to two grey square vertices, which are further connected to external lines. Coefficient: $1/2$.
- Row 3: A diagram with a central red circle vertex connected to two grey square vertices, which are further connected to external lines. Coefficient: $1/4$.
- Row 4: A diagram with a central red circle vertex connected to two grey square vertices, which are further connected to external lines. Coefficient: $1/4$.
- Row 5: A diagram with a central black circle vertex connected to four grey square vertices, which are further connected to external lines. Coefficient: $1/8$.
- Row 6: A diagram with a central black circle vertex connected to four grey square vertices, which are further connected to external lines. Coefficient: $1/2$.

The diagrams are labeled with $\bar{V}^{(4)}$ in some cases, indicating a four-point vertex function. The entire set of diagrams is labeled (88).

Even though many of the diagrams vanish in the Hartree approximation, there are still quite a few to evaluate. However, before doing so explicitly, one can show that some of them only contribute at $O(\epsilon)$. This can be seen as follows: potential topologies that can contribute in any of the $\Gamma_{\text{int}}^{2\text{PI}}$ blobs that appear in loops and do not vanish is $\sim (\lambda_R + \delta\lambda_n)$, $n = 0, 2$. Due to the shifts (74), this gives a factor that is always $O(\epsilon)$. Other factors of ϵ come from the loop integrals: one- and two-point integrals are $O(\epsilon^{-1})$ and n -point functions with $n \geq 3$ are $O(1)$. Finally, the vertex function $\bar{V}^{(4)}$ is of course $O(1)$. Thus, one can count the powers of ϵ for each diagram and, as it turns out, many diagrams only contribute at $O(\epsilon)$ to the total four-point function.

This analysis can be first applied to the self-energy boxes, revealing that $\delta^n \bar{\Pi} / \delta \phi_R^n$ ($n = 1, 2, 3$) are all $O(1)$. In (87), one finds that only the second and last terms are finite and the other two non-vanishing ones give $O(\epsilon)$ contributions. In the case of (88), an analogous analysis reveals that only two contribute: the fourteenth and the last one. Finally, we return

to the four-point function (86) and applying the same analysis, we find that the first, eighth and last diagrams contribute at $O(1)$.

There are 3- and 4-point loop integrals among these diagrams which, in dimensional regularisation, are the well-known C_0 and D_0 functions

$$C_0(p_1, p_2) = (16\pi^2) \int_q G_R(q) G_R(q + p_1) G_R(q + p_2) \quad (89)$$

$$D_0(p_1, p_2, p_3) = -i(16\pi^2) \int_q G_R(q) G_R(q + p_1) G_R(q + p_2) G_R(q + p_3). \quad (90)$$

Note that both functions are ultraviolet finite and explicit expressions can be found, for example in [36].

Assembling the different contributions, with the momentum assignments $p_{1,2}$ incoming and $p_{3,4}$ outgoing, we obtain

$$\begin{aligned} \Gamma^{(4)}(p_1, p_2, p_3, p_4) = & -(\lambda_R + \delta\lambda_4) + \lambda_R [J(p_1 + p_2) + J(p_1 - p_3) + J(p_1 - p_4)] \\ & + \frac{\lambda_R^3 \phi_R^2}{16\pi^2} [J(p_1 + p_2) J(p_3) J(p_4) C_0(p_1 + p_2, p_4) + J(p_1 - p_3) J(p_2) J(p_4) C_0(p_1 - p_3, p_4) \\ & + J(p_1 - p_4) J(p_2) J(p_3) C_0(p_1 - p_4, p_3) + J(p_1) J(p_2) J(p_3 + p_4) C_0(p_1, p_3 + p_4) \\ & + J(p_1) J(p_3) J(p_2 - p_4) C_0(p_1, p_2 - p_4) + J(p_1) J(p_4) J(p_2 - p_3) C_0(p_1, p_2 - p_3)] \\ & - \frac{\lambda_R^4 \phi_R^4}{16\pi^2} J(p_1) J(p_2) J(p_3) J(p_4) [D_0(p_2, p_1 + p_2, p_3) + D_0(p_2, p_2 - p_3, p_3) + D_0(p_2, p_2 - p_4, p_4)] \\ & + \frac{\lambda_R^5 \phi_R^4}{(16\pi^2)^2} J(p_1) J(p_2) J(p_3) J(p_4) [J(p_1 + p_2) C_0(p_1, p_1 + p_2) C_0(p_3 + p_4, p_4) \\ & + J(p_1 - p_3) C_0(p_1, p_1 - p_3) C_0(p_4 - p_2, p_4) + J(p_1 - p_4) C_0(p_1, p_1 - p_4) C_0(p_3 - p_2, p_3)], \end{aligned} \quad (91)$$

where we have introduced

$$J(p) \equiv \left[1 - \frac{\lambda_R}{32\pi^2} (B_0(p_*^2, m_R^2, m_R^2) - B_0(p^2, m_R^2, m_R^2)) \right]^{-1} \quad (92)$$

which originates from the vertex function. The counterterm, $\delta\lambda_4$ can then easily be obtained by the renormalization condition (54).

For completeness, one should also note that only in the broken phase ($\phi_R \neq 0$), there exists a physical three-point function, for which we have the following topologies

$$\Gamma^{(3)} \equiv \frac{\delta^3 \Gamma}{\delta \phi^3} = \text{diagram 1} + \frac{1}{2} \text{diagram 2}$$

$$\begin{aligned}
& + \frac{1}{4} \text{ (diagram 1) } + \frac{1}{4} \text{ (diagram 2) } \\
& + \frac{1}{2} \text{ (diagram 3) } .
\end{aligned} \tag{93}$$

In this case, we work with the convention that p_1 is the incoming four-momentum and p_2 and p_3 are outgoing. One then obtains the expression

$$\begin{aligned}
\Gamma^{(3)}(p_1, p_2, p_3) = & -(\lambda_R + \delta\lambda_4)\phi_R + \frac{1}{2}\lambda_R\phi_R [J(p_1) + J(p_2) + J(p_3)] \\
& - \frac{1}{2}\lambda_R^3\phi_R^3 J(p_1)J(p_2)J(p_3) \frac{[C_0(p_1, p_2) + C_0(p_1, p_3)]}{16\pi^2} + \mathcal{O}(\epsilon), \tag{94}
\end{aligned}$$

which is fully determined from the counterterm $\delta\lambda_4$.

4.2 Scalar Sunset Approximation

Introducing a trilinear coupling, the effective action is now given by

$$\begin{aligned}
\Gamma_{\text{int}}^{2\text{PI}}[\phi_R, G_R] = & -\frac{1}{2} \int_x (\delta Z_{\phi,0} \square_x + \delta m_0^2) G_R(x, y) \Big|_{x=y} - \frac{1}{2} \int_x \phi_R(x) (\delta Z_{\phi,2} \square_x + \delta m_2^2) \phi_R(x) \\
& - \int_x \left[\frac{1}{8} (\lambda_R + \delta\lambda_0) G_R^2(x, x) + \frac{1}{4} (\lambda_R + \delta\lambda_2) G_R(x, x) \phi_R^2(x) + \frac{1}{4!} (\lambda_R + \delta\lambda_4) \phi_R^4(x) \right] \\
& - \int_x \delta t_1 \phi_R(x) - \int_x \left[\frac{1}{2} (\alpha_R + \delta\alpha_1) \phi_R(x) G_R(x, x) + \frac{1}{3!} (\alpha_R + \delta\alpha_3) \phi_R^3(x) \right] \\
& + \frac{i}{12} \int_x \int_y [(\alpha_R + \delta\alpha_0) + (\lambda_R + \delta\lambda_1) \phi(x)] [(\alpha_R + \delta\alpha_0) + (\lambda_R + \delta\lambda_1) \phi(y)] G_R^3(x, y) \tag{95}
\end{aligned}$$

In this case, we carry out the renormalization at non-vanishing field expectation value $\phi_R \neq 0$, as there is no symmetry in the model.

We may set the counterterms, $\delta\alpha_0 = \delta\lambda_1 = 0$, which is possible as they amount to finite renormalizations at this level of the 2PI truncation; more specifically, the first non-trivial contribution to these are obtained when one includes the basketball diagram [21, 23, 24]. We then obtain the following four-point kernels which are now momentum dependent

$$\bar{\Lambda}^{(4)}(p_1, p_2, p_3, p_4) = -(\lambda_R + \delta\lambda_0) + 2i(\alpha_R + \lambda_R\phi_R)^2 G_R(p_3 - p_1), \tag{96}$$

$$\Lambda^{(4)}(p_1, p_2, p_3, p_4) = -(\lambda_R + \delta\lambda_2) + i\lambda_R^2 \int_q G_R(q) G_R(p + q)$$

$$\equiv -(\lambda_R + \delta\lambda_2) + \lambda_R^2 \mathcal{I}(p), \quad (97)$$

where $p = p_1 + p_2$. In addition, we also define the following three-point kernel

$$\Lambda^{(3)}(p_1, p_2, p_3) = 2 \frac{\delta^2 \Gamma_{\text{int}}^{2\text{PI}}}{\delta\phi_R \delta G_R(p_1)} = -(\alpha_R + \delta\alpha_1) + \lambda_R(\alpha_R + \lambda_R\phi_R) \mathcal{I}(p_1). \quad (98)$$

The corresponding BSE for its resummation is

$$\begin{aligned} V^{(3)}(p_1, p_2, p_3) &= \Lambda^{(3)}(p_1, p_2, p_3) \\ &+ \frac{i}{2} \int_q \Lambda^{(3)}(p_1, p_2, p_3) G_R(q) G_R(p_1 + q) \bar{V}^{(4)}(q + p_1, -q, p_2, p_3). \end{aligned} \quad (99)$$

We now implement appropriate renormalization conditions in order to determine the various coupling constant counterterms. For the four-point vertices, we continue to work with the convention that we have $p_{1,2}$ as incoming and $p_{3,4}$ as outgoing momenta. We first have from (36),

$$\begin{aligned} \bar{V}^{(4)}(p_1, p_2, p_3, p_4) &= \bar{\Lambda}^{(4)}(p_1, p_2, p_3, p_4) \\ &+ \frac{i}{2} \int_q \bar{\Lambda}^{(4)}(p_1, p_2, q + p, -q) G_R(q) G_R(p + q) \bar{V}^{(4)}(q + p, -q, p_3, p_4). \end{aligned} \quad (100)$$

Let us set the renormalization condition,

$$\bar{V}^{(4)}(p_{1*}, p_{2*}, p_{3*}, p_{4*}) = -\lambda_R + 2i(\alpha_R + \lambda_R\phi_R)^2 G_R(p_{3*} - p_{1*}), \quad (101)$$

which accounts for the fact that four scalars may scatter directly via the quartic coupling, or by a scalar exchange through two trilinear couplings. Like in the Hartree approximation, we work in the COM system, which is characterised by a COM momentum and scattering angle. In this case, the second term induces a dependence on the scattering angle and, thus, we set $|\vec{p}_*| = m_R$ and $\theta_* = \pi$ as our renormalization point. Using (101) and solving for $\delta\lambda_0$, we obtain

$$\delta\lambda_0 = -\lambda_R + \frac{\lambda_R - (\alpha_R + \lambda_R\phi_R)^2 I_2(p_*, p_{2*}, p_{3*}, p_{4*})}{1 + \frac{1}{2} I_1(p_*, p_{3*}, p_{4*})}, \quad (102)$$

where we have defined the following integrals over the vertex functions:

$$I_1(p, k, r) = i \int_q G_R(q) G_R(p + q) \bar{V}^{(4)}(q + p, -q, k, r), \quad (103)$$

$$I_2(p, k, r, l) = \int_q G_R(q) G_R(q + p) G_R(q + k) G_R(q + r) \bar{V}^{(4)}(q + p, -q, r, l). \quad (104)$$

Note that the functions I_1 and I_2 are at most logarithmically divergent and finite respectively, which we can ascertain by counting the number of propagators involved. The counterterm

$\delta\lambda_0$ from (102) is hence discerned as finite. Plugging this back into (96) and (100), we obtain the following expression for the four-point function

$$\begin{aligned} \bar{V}^{(4)}(p_1, p_2, p_3, p_4) &= -\lambda_R \left(\frac{1 + \frac{1}{2}I_1(p, p_3, p_4)}{1 + \frac{1}{2}I_1(p_*, p_{3*}, p_{4*})} \right) + 2i(\alpha_R + \lambda_R\phi_R)^2 G_R(p_3 - p_1) \\ &+ (\alpha_R + \lambda_R\phi_R)^2 \left[I_2(p, p_2, p_3, p_4) - I_2(p_*, p_{3*}, p_{4*}) \left(\frac{1 + \frac{1}{2}I_1(p, p_3, p_4)}{1 + \frac{1}{2}I_1(p_*, p_{3*}, p_{4*})} \right) \right], \end{aligned} \quad (105)$$

which is discerned to be finite from the arguments related to the loop integrals presented above.

As our model does not possess the \mathbb{Z}_2 symmetry in the Hartree case, our starting point to determine the counterterm $\delta\lambda_2$ is the following BSE

$$\begin{aligned} V^{(4)}(p_1, p_2, p_3, p_4) &= \Lambda^{(4)}(p_1, p_2, p_3, p_4) \\ &+ \frac{i}{2} \int_q \Lambda^{(4)}(p_1, p_2, q + p, -q) G_R(q) G_R(q + p) \bar{V}^{(4)}(q + p, -q, p_3, p_4). \end{aligned} \quad (106)$$

From the definition (97), $\Lambda^{(4)}$ does not depend on the integrating loop momentum, which simplifies matters. We impose the renormalization condition

$$V^{(4)}(p_{1*}, p_{2*}, p_{3*}, p_{4*}) = -\lambda_R \quad (107)$$

and this leads to the following result

$$\delta\lambda_2 = -\lambda_R + \lambda_R^2 \mathcal{I}(p_*) + \frac{\lambda_R}{1 + \frac{1}{2}I_1(p_*, p_{3*}, p_{4*})}. \quad (108)$$

Firstly, we notice that $\delta\lambda_2 \neq \delta\lambda_0$ unlike in the Hartree approximation, even if we set $\alpha = 0$. This is because, in the scalar sunset approximation, the effective trilinear coupling $\sim \lambda_R\phi_R$ gives a contribution which is the second term of (108). The very same term introduces a divergence in $\delta\lambda_2$ due to the loop integral $\mathcal{I}(p) = i \int_q G_R(q) G_R(q + p)$.

We now examine the three-point function (99), which has a similar structure to $V^{(4)}$. Firstly, let us describe the kinematics: we take two of the scalars with four-momenta p_2 and p_3 to be on-shell. By the conservation of four-momentum, we can calculate p_1 as

$$p_1^2 = (p_2 + p_3)^2 = 4(|\vec{p}|^2 + m_R^2), \quad (109)$$

where we work in the COM frame for p_2 and p_3 so that these scalars are produced back-to-back. For our renormalization condition, we fix the four vectors as follows

$$p_{2*} = \left[\sqrt{2}m_R, \vec{p}_* \right], \quad p_{3*} = \left[\sqrt{2}m_R, -\vec{p}_* \right], \quad p_{1*} = \left[2\sqrt{2}m_R, 0 \right] \quad (110)$$

with $|\vec{p}_*| = m_R$ and require

$$V^{(3)}(p_{1*}, p_{2*}, p_{3*}) = -\alpha_R. \quad (111)$$

This gives us the following relation

$$\delta\alpha_1 = -\alpha_R + \lambda_R(\alpha_R + \lambda_R\phi_R)\mathcal{I}(p_{1*}^2) + \frac{\alpha_R}{1 + \frac{1}{2}I_1(p_{1*}, p_{2*}, p_{3*})}. \quad (112)$$

This counterterm is also divergent for the same reason as $\delta\lambda_2$.

Turning now to the gap equation, with p being the external momentum, this reads

$$\begin{aligned} iG_R^{-1}(p) &= (p^2 - m_R^2) + (\delta Z_{\phi,0} p^2 - \delta m_0^2) - (\alpha_R + \delta\alpha_1)\phi_R - \frac{(\lambda_R + \delta\lambda_2)}{2}\phi_R^2 \\ &\quad - \frac{(\lambda_R + \delta\lambda_0)}{2}\mathcal{T} + \frac{(\alpha_R + \lambda_R\phi_R)^2}{2}\mathcal{I}(p), \end{aligned} \quad (113)$$

where we have the one-point integral

$$\mathcal{T} = \int_q G_R(q). \quad (114)$$

Using the same on-shell renormalization conditions in the Hartree approximation, as defined in (67) and (68), we first pick up a finite contribution to the wave function renormalization given by

$$\delta Z_{\phi,0} = -\frac{(\alpha_R + \lambda_R\phi_R)^2}{2} \frac{\partial \mathcal{I}(p)}{\partial p^2} \Big|_{p^2=m_R^2}. \quad (115)$$

The derivative eliminates any divergence present and therefore, $\delta Z_{\phi,0}$ is finite in the scalar sunset approximation. We can then determine the mass counterterm

$$\begin{aligned} \delta m_0^2 &= \delta Z_{\phi,0} m_R^2 - (\alpha_R + \delta\alpha_1)\phi_R - \frac{(\lambda_R + \delta\lambda_2)}{2}\phi_R^2 - \frac{(\lambda_R + \delta\lambda_0)}{2}\mathcal{T} \\ &\quad + \frac{(\alpha_R + \lambda_R\phi_R)^2}{2}\mathcal{I}(p) \Big|_{p^2=m_R^2}. \end{aligned} \quad (116)$$

This counterterm is no longer finite like in the Hartree approximation: the reason for this is that we have noted that the counterterms $\delta\lambda_2$ and $\delta\alpha_1$ are divergent. We plug back δm_0^2 and $\delta Z_{\phi,0}$ into (113) to obtain the following integral equation to ascertain the propagator

$$iG_R^{-1}(p) = (p^2 - m_R^2) \left[1 - \frac{(\alpha_R + \lambda_R\phi_R)^2}{2} \frac{\partial \mathcal{I}(q)}{\partial q^2} \Big|_{q^2=m_R^2} \right] + \frac{(\alpha_R + \lambda_R\phi_R)^2}{2} \left[\mathcal{I}(p) - \mathcal{I}(q) \Big|_{q^2=m_R^2} \right]. \quad (117)$$

In this form, the propagator is manifestly finite due to potential divergences dropping out in the difference of the loop integral \mathcal{I} or in its differentiation. However, G_R cannot be given in an explicit form but needs to be determined by solving (117), for which we use an iterative approach, described as follows:

1. Initialising with the free propagator, we evaluate the loop integrals in (117) to yield the first iteration of the propagator in terms of Passarino-Veltman functions

$$i(G_R^{-1}(p))^{(0)} = (p^2 - m_R^2) \left[1 - \frac{(\alpha_R + \lambda_R \phi_R)^2}{32\pi^2} \dot{B}_0(m_R^2, m_R^2, m_R^2) \right] + \frac{(\alpha_R + \lambda_R \phi_R)^2}{32\pi^2} [B_0(p^2, m_R^2, m_R^2) - B_0(m_R^2, m_R^2, m_R^2)] . \quad (118)$$

2. For the next iteration, convert (118) to Euclidean space. Then, use a numerical implementation of the loop integral $\mathcal{I}(p)$ given as [23]

$$\int_q G_R^E(\|q\|) G_R^E(\|p+q\|) = \frac{1}{8\pi^3 p^2} \int_0^\Lambda dq q G_R^E(q) \int_{|(q-|p||}^{\min\{|(q+|p||), \Lambda\}} du u \sqrt{-\lambda(u^2, q^2, \|p\|^2)} G_R^E(u) , \quad (119)$$

where the superscript E denotes Euclidean propagators and the momenta are in Euclidean space. We denote $\lambda(x, y, z) = x^2 + y^2 + z^2 - 2xy - 2yz - 2zx$ as the Källén function and $\|x\|$ as the Euclidean norm of x . Finally, Λ denotes the UV cutoff which, in principle, tends to infinity, but for our numerical implementation needs to be sufficiently large as compared to the scalar mass, the only relevant mass scale.

3. Generate a set of points for this iteration of the propagator and interpolate these to obtain the propagator at this iteration.
4. Repeat now from step (2) until the iteration converges to the desired accuracy. As a criterion, we use the relative difference between successive iterations.

Our results in Fig. 3 show that there is indeed convergence for this iterative procedure as relative differences between successive iterations continue to get smaller for the very large couplings chosen. It would suffice, for smaller couplings hence, to use the first iteration of the propagator for practical purposes. We have also checked the dependence on the UV cutoff, Λ , and find it to be rather small, with the relative difference being at most $\mathcal{O}(10^{-5})$, even when choosing a cutoff two orders of magnitude higher.

For the determination of the remaining counterterms, we examine various derivatives of the 2PI effective potential. For example, the tadpole counterterm is straightforwardly obtained by taking a single derivative of the effective action w.r.t. ϕ_R . The stationarity condition then gives

$$\Gamma^{(1)} = -\delta t_1 - (m_R^2 + \delta m_2^2) \phi_R - \frac{(\alpha_R + \delta \alpha_3)}{2} \phi_R^2 - \frac{(\alpha_R + \delta \lambda_4)}{6} \phi_R^2 - \frac{1}{2} [(\alpha_R + \delta \alpha_1) + (\lambda_R + \delta \lambda_4) \phi_R] \mathcal{T} + \frac{\lambda_R (\alpha_R + \lambda_R \phi_R)}{6} \mathcal{S} \stackrel{!}{=} 0 , \quad (120)$$

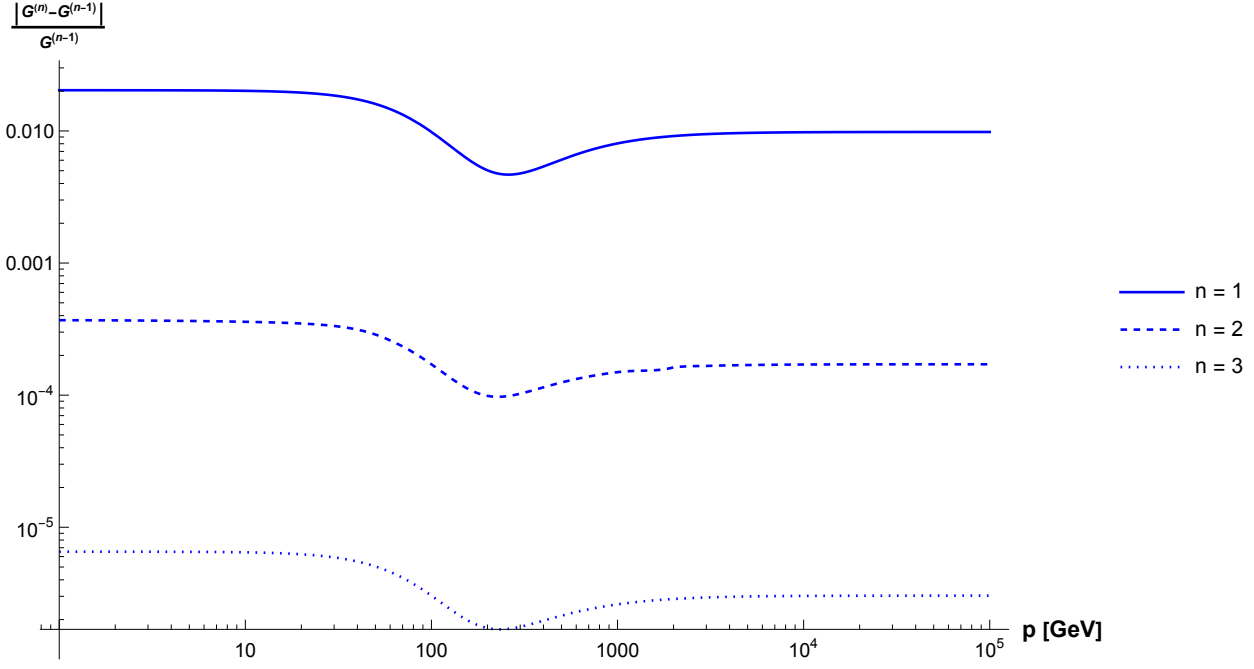


Figure 3: The relative difference between successive iterations of the scalar propagator for parameter choices of $m_R = 100$ GeV, $\alpha_R = 200$ GeV and $\lambda_R = 4$, leading to $\phi_R \approx 70$ GeV for a range of the norm of the Euclidean four-momentum \mathbf{p} . We chose the UV cutoff $\Lambda = 10^6$ GeV, as explained in the text.

where

$$\mathcal{S} = i \int_p \int_q G_R(p) G_R(q) G_R(p+q). \quad (121)$$

The tadpole counterterm cannot be determined without first ascertaining the missing field counterterms. The easiest of these to find is δm_2^2 , for which we look at $\Gamma^{(2)}$. Using equations (79) and (81) we obtain

$$\begin{aligned} \Gamma^{(2)}(p) = & (p^2 - m_R^2) + (\delta Z_{\phi,2} p^2 - \delta m_2^2) - (\alpha_R + \delta\alpha_3)\phi_R - \frac{1}{2}(\lambda_R + \delta\lambda_4)\phi_R^2 \\ & - \frac{1}{2}(\lambda_R + \delta\lambda_2)\mathcal{T} + \frac{\lambda_R^2}{6}\mathcal{S} \\ & - \frac{1}{8} \left[(\alpha_R + \delta\alpha_1) + (\lambda_R + \delta\lambda_2)\phi_R - \frac{\lambda_R(\alpha_R + \lambda_R\phi_R)}{3}\mathcal{I}(p) \right]^2 \mathcal{I}(p) \\ & + \frac{1}{16} \left\{ \left[(\alpha_R + \delta\alpha_1) + (\lambda_R + \delta\lambda_2)\phi_R - \frac{\lambda_R(\alpha_R + \lambda_R\phi_R)}{3}\mathcal{I}(p) \right]^2 \right. \\ & \left. \int_q \int_k G_R(p+q) G_R(q) \bar{V}^{(4)}(p+q, -q, p+k, -k) G_R(p+k) G_R(k) \right\}, \quad (122) \end{aligned}$$

where the terms in parenthesis for the third and last lines appear from the replacement of the various building blocks in (79) and (81). The earlier analysis in the Hartree approximation does not carry over as $\delta\lambda_2 \neq \delta\lambda_0$, and moreover, $\delta\lambda_2$ is now contains a divergent part. We can determine the counterterms $\delta Z_{\phi,2}$ and δm_2^2 with the on-shell renormalization conditions, to give

$$\begin{aligned} \delta Z_{\phi,2} &= \frac{1}{8} \left[(\alpha_R + \delta\alpha_1) + (\lambda_R + \delta\lambda_2)\phi_R - \frac{\lambda_R(\alpha_R + \lambda_R\phi_R)}{3} \mathcal{I}(p) \Big|_{p^2=m_R^2} \right] \\ &\left\{ \left\{ - \frac{\lambda_R(\alpha_R + \lambda_R\phi_R)}{3} \mathcal{I}(p) \Big|_{p^2=m_R^2} \frac{\partial \mathcal{I}(p)}{\partial p^2} \Big|_{p^2=m_R^2} \right. \right. \\ &\quad \left. \left. + \left[(\alpha_R + \delta\alpha_1) + (\lambda_R + \delta\lambda_2)\phi_R - \frac{\lambda_R(\alpha_R + \lambda_R\phi_R)}{3} \mathcal{I}(p) \Big|_{p^2=m_R^2} \right] \frac{\partial \mathcal{I}(p)}{\partial p^2} \Big|_{p^2=m_R^2} \right\} \right. \\ &+ \frac{1}{2} \left\{ - \frac{\lambda_R(\alpha_R + \lambda_R\phi_R)}{3} \mathcal{I}(p) \Big|_{p^2=m_R^2} \frac{\partial \mathcal{I}_V(p)}{\partial p^2} \Big|_{p^2=m_R^2} \right. \\ &\quad \left. \left. + \left[(\alpha_R + \delta\alpha_1) + (\lambda_R + \delta\lambda_2)\phi_R - \frac{\lambda_R(\alpha_R + \lambda_R\phi_R)}{3} \mathcal{I}(p) \Big|_{p^2=m_R^2} \right] \frac{\partial \mathcal{I}_V(p)}{\partial p^2} \Big|_{p^2=m_R^2} \right\} \right\}, \quad (123) \end{aligned}$$

$$\begin{aligned} \delta m_2^2 &= m_R^2 \delta Z_{\phi,2} - (\alpha_R + \delta\alpha_3)\phi_R - \frac{1}{2}(\lambda_R + \delta\lambda_4)\phi_R^2 - \frac{1}{2}(\lambda_R + \delta\lambda_2)\mathcal{T} + \frac{\lambda_R^2}{6} \mathcal{S} \\ &- \frac{1}{8} \left[(\alpha_R + \delta\alpha_1) + (\lambda_R + \delta\lambda_2)\phi_R - \frac{\lambda_R(\alpha_R + \lambda_R\phi_R)}{3} \mathcal{I}(p) \Big|_{p^2=m_R^2} \right]^2 \mathcal{I}(p) \Big|_{p^2=m_R^2} \\ &+ \frac{1}{16} \left[(\alpha_R + \delta\alpha_1) + (\lambda_R + \delta\lambda_2)\phi_R - \frac{\lambda_R(\alpha_R + \lambda_R\phi_R)}{3} \mathcal{I}(p) \Big|_{p^2=m_R^2} \right]^2 \mathcal{I}_V(p) \Big|_{p^2=m_R^2}, \quad (124) \end{aligned}$$

where

$$\mathcal{I}_V(p) = \int_q \int_k G_R(p+q) G_R(q) \bar{V}^{(4)}(p+q, -q, p+k, -k) G_R(p+k) G_R(k). \quad (125)$$

On close inspection, we can discern that these counterterms would not be finite like in the Hartree approximation, due to the coupling constant counterterms being $\mathcal{O}(\epsilon^{-1})$. Furthermore, it is also obvious that the equalities $\delta Z_{\phi,2} = \delta Z_{\phi,0}$ and $\delta m_2^2 = \delta m_0^2$ no longer hold true, as we had in the Hartree approximation.

Finally, the only undetermined counterterms are $\delta\alpha_3$ and $\delta\lambda_4$, which are needed to completely express δt_1 and δm_2^2 . The corresponding formulas are very lengthy and, thus we give here the corresponding diagrammatic representation.

$$\Gamma^{(3)} \equiv \frac{\delta^3 \Gamma}{\delta \phi^3} = \begin{array}{c} \text{Diagram 1} \\ \text{Diagram 2} \\ \text{Diagram 3} \\ \text{Diagram 4} \end{array} + \frac{1}{2} \begin{array}{c} \text{Diagram 5} \\ \text{Diagram 6} \end{array} + \frac{1}{4} \begin{array}{c} \text{Diagram 7} \\ \text{Diagram 8} \end{array} + \begin{array}{c} \text{Diagram 9} \\ \text{Diagram 10} \end{array}$$

$$+ \frac{1}{2} \text{diagram} . \quad (126)$$

$$\Gamma^{(4)} \equiv \frac{\delta^4 \Gamma}{\delta \phi^4} = \text{diagram} + \frac{1}{4} \text{diagram} + \frac{1}{8} \text{diagram} + \text{diagram} + \frac{1}{2} \text{diagram} + \text{diagram} + \frac{1}{2} \text{diagram} + \frac{1}{4} \text{diagram} + \text{diagram} + \frac{1}{2} \text{diagram} . \quad (127)$$

Referring now to (87) and (88), we first enlist the various non-vanishing contributions of the derivative of the self-energy w.r.t. ϕ_R that would be required.

$$\text{diagram} = \text{diagram} + \frac{1}{2} \text{diagram} + \frac{1}{2} \text{diagram} + \frac{1}{4} \text{diagram}$$

$$\begin{aligned}
& + \frac{1}{4} \begin{array}{c} \square \bullet \square \circ \\ | \quad | \\ \square \\ | \\ \circ \end{array} + \frac{1}{8} \begin{array}{c} \square \overline{V}^{(4)} \bullet \square \circ \\ | \quad | \\ \square \\ | \\ \circ \end{array} \\
& + \begin{array}{c} \square \bullet \square \circ \\ | \quad / \\ \square \\ | \\ \circ \end{array} + \frac{1}{2} \begin{array}{c} \square \overline{V}^{(4)} \bullet \square \circ \\ | \quad / \\ \square \\ | \\ \circ \end{array} \\
\begin{array}{c} \square \circ \\ | \\ \square \circ \end{array} = & + \frac{1}{4} \begin{array}{c} \square \bullet \square \circ \\ | \quad | \\ \square \\ | \\ \circ \end{array} + \frac{1}{8} \begin{array}{c} \square \overline{V}^{(4)} \bullet \square \circ \\ | \quad | \\ \square \\ | \\ \circ \end{array} \\
& + \frac{1}{8} \begin{array}{c} \square \bullet \square \circ \\ | \quad | \\ \square \\ | \\ \circ \end{array} + \frac{1}{16} \begin{array}{c} \square \overline{V}^{(4)} \bullet \square \circ \\ | \quad | \\ \square \\ | \\ \circ \end{array} \\
& + \begin{array}{c} \square \bullet \square \circ \\ | \quad / \\ \square \\ | \\ \circ \end{array} + \frac{1}{2} \begin{array}{c} \square \overline{V}^{(4)} \bullet \square \circ \\ | \quad / \\ \square \\ | \\ \circ \end{array} \\
& + \frac{1}{2} \begin{array}{c} \square \bullet \square \circ \\ | \quad | \\ \square \\ | \\ \circ \end{array} + \frac{1}{4} \begin{array}{c} \square \overline{V}^{(4)} \bullet \square \circ \\ | \quad | \\ \square \\ | \\ \circ \end{array}
\end{aligned}
\tag{128}$$

$$\begin{aligned}
& + \text{[Diagram 1]} + \frac{1}{2} \text{[Diagram 2]} \\
& + \frac{1}{2} \text{[Diagram 3]} + \frac{1}{4} \text{[Diagram 4]} \\
& + \frac{1}{4} \text{[Diagram 5]} + \frac{1}{8} \text{[Diagram 6]} \\
& + \text{[Diagram 7]} + \frac{1}{2} \text{[Diagram 8]} .
\end{aligned} \tag{129}$$

While performing the analysis of the diagrams, one may note the following: $\delta\lambda_0$ is still finite and differentiation w.r.t. to three propagators yields $\sim (\alpha_R + \lambda_R\phi_R)^2$ which is also finite. However, all other counterterms, besides $\delta\lambda_0$ are not finite, and hence one needs to be careful when such quantities multiply divergent loop integrals. The explicit form of the counterterms $\delta\alpha_3$ and $\delta\lambda_4$ are obtained by placing the renormalization conditions

$$\Gamma^{(3)}(p_{1*}, p_{2*}, p_{3*}) = -\alpha_R, \quad \Gamma^{(4)}(p_{1*}, p_{2*}, p_{3*}, p_{4*}) = -\lambda_R. \tag{130}$$

For the numerical evaluation of the three- and four-point functions, one can then use the same numerical procedure as outlined above for G .

5 Fermionic Sunset Approximation

Including fermions, we obtain the following effective action

$$\begin{aligned}
\Gamma_{\text{int}}^{2\text{PI}}[\phi_R, G_R, D_R] &= -\frac{1}{2} \int_x (\delta Z_{\phi,0} \square_x + \delta m_0^2) G_R(x, y) \Big|_{x=y} - \frac{1}{2} \int_x \phi_R(x) (\delta Z_{\phi,2} \square_x + \delta m_2^2) \phi_R(x) \\
&- \int_x \left[\frac{1}{8} (\lambda_R + \delta \lambda_0) G_R^2(x, x) + \frac{1}{4} (\lambda_R + \delta \lambda_2) G_R(x, x) \phi_R^2(x) + \frac{1}{4!} (\lambda_R + \delta \lambda_4) \phi_R^4(x) \right] \\
&- \int_x \left[\frac{1}{2} (\alpha_R + \delta \alpha_1) \phi_R(x) G_R(x, x) + \frac{1}{3!} (\alpha_R + \delta \alpha_3) \phi_R^3(x) \right] \\
&+ \frac{i}{12} \int_x \int_y (\alpha_R + \lambda_R \phi(x)) (\alpha_R + \lambda_R \phi(y)) G_R^3(x, y) \\
&+ \int_x (i \delta Z_{\psi,0} \not{\partial}_x - \delta M_0) D_R(x, y) \Big|_{x=y} \\
&- \frac{i}{2} \int_x \int_y (g_R + \delta g_0)^2 G_R(x, y) \text{tr}[D_R(x, y) D_R(y, x)] - \int_x \delta t_1 \phi_R(x) \\
&- \int_x [(g_R + \delta g_1) \phi_R(x) \text{tr}[D_R(x, x)]] . \tag{131}
\end{aligned}$$

where we have already set the corresponding coupling counterterms for the scalar sunset contribution to 0. We retain the counterterm for the Yukawa coupling corresponding to the fermionic sunset diagram, δg_0 , for the moment. Note that as long as the fermionic mass M_R does not vanish, we require an additional trilinear coupling α_R to account for potential divergences in scalar three-point functions with a fermionic loop. We can then obtain the following additional kernels involving fermions and scalars [30]

$$\Lambda_{\psi\psi}(p_1, p_2, p_3, p_4)_{ab,cd} \equiv -\frac{\delta^2 \Gamma_{\text{int}}^{2\text{PI}}}{\delta D_R^{ba}(p) \delta D_R^{cd}(q)} = i(g_R + \delta g_0)^2 \delta_{ab} G_R(p_3 - p_1) \delta_{ac}, \tag{132}$$

$$\Lambda_{\psi\phi}^{(4)}(p_1, p_2, p_3, p_4)_{ab} \equiv -2 \frac{\delta^2 \Gamma_{\text{int}}^{2\text{PI}}}{\delta D_R^{ba}(p) \delta G_R(q)} = 2i(g_R + \delta g_0)^2 D_R(p_1 - p_3)_{ab}, \tag{133}$$

$$\left(\Lambda_{\psi\phi}^{(3)} \right)_{ab} \equiv -\frac{\delta^2 \Gamma_{\text{int}}^{2\text{PI}}}{\delta \phi_R \delta D_R^{ba}(p)} = -(g_R + \delta g_1) \delta_{ab}, \tag{134}$$

alongside the scalar kernels that we had in the scalar sunset approximation, c.f. (96), (97) and (98). For now, we have denoted the spinor indices by lowercase Latin characters. The Kronecker deltas refer to the identity matrix in spinor space.

We proceed by defining first the governing BSE for the kernel $\Lambda_{\psi\psi}$ as

$$V_{\psi\psi}(p_1, p_2, p_3, p_4)_{ab,cd} = \Lambda_{\psi\psi}(p_1, p_2, p_3, p_4)_{ab,cd}$$

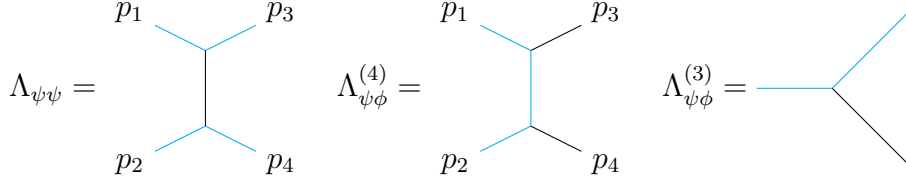


Figure 4: Illustration of the various kernels in the fermionic sunset approximation. Cyan lines indicate the fermionic propagator D_R .

$$\begin{aligned}
& + i \int_q \Lambda_{\psi\psi}(p_1, p_2, q+p, -q)_{ab,ef} D_R(q)_{eg} V_{\psi\psi}(q+p, -q, p_3, p_4)_{gh,cd} D_R(p+q)_{hf} \\
& = i(g_R + \delta g_0)^2 \delta_{db} G_R(p_3 - p_1) \delta_{ac} \\
& \quad - (g_R + \delta g_0)^2 \int_q G_R(q+p_2) D_R(q)_{ae} V_{\psi\psi}(q+p, -q, p_3, p_4)_{ef,cd} D_R(p+q)_{fb}, \quad (135)
\end{aligned}$$

and $p = p_1 + p_2$. This vertex function is essentially a resummation of ladder diagrams contributing to t -channel $\psi\bar{\psi} \rightarrow \psi\bar{\psi}$ scattering via the exchange of a scalar propagator. On inspection, we can easily discern that $V_{\psi\psi}$ is finite by counting the number of propagators. The counterterm δg_0 hence accounts for a finite renormalization which we determine using the condition

$$V_{\psi\psi}(p_{1*}, p_{2*}, p_{3*}, p_{4*})_{ab,cd} = i g_R^2 \delta_{db} G_R(p_{3*} - p_{1*}) \delta_{ac}. \quad (136)$$

where we continue to work in the COM frame to give the renormalization conditions. Imposing this and appropriately contracting the spinor indices (with $\sum_a \delta_{aa} = 4$) we obtain the following expression for δg_0

$$\delta g_0 = -g_R + \frac{g_R}{\sqrt{1 - \frac{1}{4} G_R^{-1}(p_{3*} - p_{1*}) F_2}} \quad (137)$$

where

$$F_2 = i \int_q G_R(q+p_{2*}) D_R(q)_{ae} V_{\psi\psi}(q+p_*, -q, p_{3*}, p_{4*})_{ef,ab} D_R(p_*+q)_{fb}. \quad (138)$$

Note that δg_0 is a finite renormalization, i.e. $\mathcal{O}(1)$ and therefore, does not modify divergent structures. Thus, for convenience, we choose to set $\delta g_0 = 0$ from this point onward.

Let us consider the BSE for the kernel $\Lambda_{\psi\phi}^{(4)}$,

$$\begin{aligned}
V_{\psi\phi}^{(4)}(p_1, p_2, p_3, p_4)_{ab} & = \Lambda_{\psi\phi}(p_1, p_2, p_3, p_4)_{ab} \\
& + i \int_q \Lambda_{\psi\phi}^{(4)}(p_1, p_2, q+p, -q)_{ae} D_R(q)_{ef} V_{\psi\phi}^{(4)}(q+p, -q, p_3, p_4)_{fb} G_R(p+q) \quad (139)
\end{aligned}$$

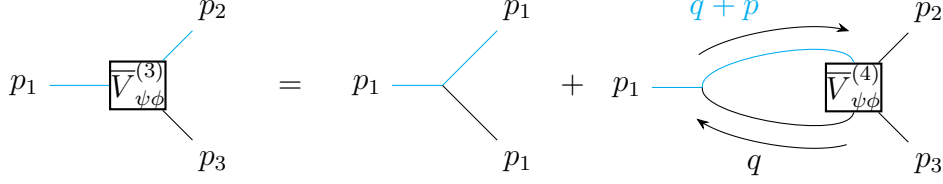


Figure 5: Illustration of BSE for the resummation of the three-point vertex $\bar{V}_{\psi\phi}^{(3)}$ using the four-point vertex $\bar{V}_{\psi\phi}^{(4)}$.

This is again finite by power counting. We will use this now for the three-point kernel $\Lambda_{\psi\phi}^{(3)}$ to define a BSE of the form

$$V_{\psi\phi}^{(3)}(p_1, p_2, p_3)_{ab} = \left(\Lambda_{\psi\phi}^{(3)}\right)_{ab} + i \left(\Lambda_{\psi\phi}^{(3)}\right)_{ac} \int_q D_R(q)_{cd} V_{\psi\phi}^{(4)}(q + p_1, -q, p_2, p_3)_{db} G_R(p_1 + q). \quad (140)$$

We will make use of this now to determine the counterterm δg_1 . With the renormalization condition

$$V_{\psi\phi}^{(3)}(p_{1*})_{(\alpha\beta)} = -g_R \delta_{\alpha\beta} \quad (141)$$

we then obtain

$$\delta g_1 = -g_R + \frac{g_R}{1 + \frac{1}{4}F_3}, \quad (142)$$

where

$$F_3 = i \int_q \text{tr} \left[D_R(q) V_{\psi\phi}^{(4)}(q + p_{1*}, -q, p_{2*}, p_{3*}) \right] G_R(q + p_{1*}), \quad (143)$$

and where appropriate contraction of the spinor indices leads to the resultant trace.

In dealing with the scalar four-point vertex functions, we have to treat the possibility of divergences introduced by fermionic loops. To this end, with $\bar{\Lambda}^{(4)}$ as the base, we build the following “modified scalar kernel” using $\Lambda_{\psi\phi}^{(4)}$ and the four-point vertex $V_{\psi\psi}$

$$\begin{aligned} \tilde{\Lambda}_{\phi\phi}(p_1, p_2, p_3, p_4) &= \bar{\Lambda}^{(4)}(p_1, p_2, p_3, p_4) \\ &\quad - i \int_q D_R(p + q)_{db} \Lambda_{\psi\phi}^{(4)}(q + p, -q, p_3, p_4)_{ba} D_R(q)_{ac} \Lambda_{\psi\phi}^{(4)}(p_1, p_2, p + q - q)_{cd} \\ &\quad + i \int_q \int_r \left\{ D_R(q + p)_{fb} \Lambda_{\psi\phi}^{(4)}(p_1, p_2, p + q, -q)_{ba} D_R(q)_{ae} \right. \\ &\quad \left. V^{\psi\psi}(p + q, -q, r + p, -r)_{ef,gh} D_R(r)_{gc} \Lambda_{\psi\phi}^{(4)}(r + p, -r, p_3, p_4)_{cd} D_R(r + p)_{dh} \right\} \\ &= \bar{\Lambda}^{(4)}(p_1, p_2, p_3, p_4) - 4i g_R^4 \int_q \text{tr} [D_R(q + p) D_R(q + p_1) D_R(q) D_R(q + p_3)] \end{aligned}$$

$$\begin{aligned}
& + 4ig_R^4 \int_q \int_r \text{tr} \left[D_R(q+p) D_R(q+p_1) D_R(q) V^{\psi\psi}(p+q, -q, r+p, -r) \right. \\
& \qquad \qquad \qquad \left. D_R(r) D_R(r+p_3) D_R(r) \right], \tag{144}
\end{aligned}$$

where in the second equality, we have contracted the spinor indices to obtain the trace. We can now iterate this four-point scalar kernel via its usual BSE

$$\begin{aligned}
\bar{V}^{(4)}(p_1, p_2, p_3, p_4) &= \tilde{\Lambda}_{\phi\phi}(p_1, p_2, p_3, p_4) \\
&+ \frac{i}{2} \int_q \tilde{\Lambda}_{\phi\phi}(p_1, p_2, q+p, -q) G_R(q) G_R(p+q) \bar{V}^{(4)}(q+p, -q, p_3, p_4). \tag{145}
\end{aligned}$$

The quartic scalar coupling divergences generated will then be absorbed into the counterterm $\delta\lambda_0$. Imposing the same renormalization condition as in the scalar sunset approximation, c.f. (101), we solve for the counterterm to obtain

$$\begin{aligned}
\delta\lambda_0 &= -\lambda_R + \frac{\lambda_R - (\alpha_R + \lambda_R\phi_R)^2 I_2}{1 + \frac{1}{2}I_1} \\
&+ 4g_R^4 \left[\frac{F_4 - \frac{1}{2}F_{4V}}{1 + \frac{1}{2}I_1} \right] - 4g_R^4 \left[\frac{F_V - \frac{1}{2}F_{VV}}{1 + \frac{1}{2}I_1} \right], \tag{146}
\end{aligned}$$

where $I_{1,2}$ are the same integrals in (103) and (104), defined at the renormalization point, and the following notation has been introduced for the new loop integrals pertaining to the fermions

$$F_4 = i \int_q \text{tr} [D_R(q+p_*) D_R(q+p_{2*}) D_R(q) D_R(q+p_{4*})], \tag{147}$$

$$F_{4V} = \int_q \int_r \text{tr} [D_R(q+p_*) D_R(q+p_{2*}) D_R(q) D_R(q-r)] G_R(r) G_R(p_*+r) \bar{V}^{(4)}(r+p_*, p_{3*}), \tag{148}$$

$$\begin{aligned}
F_V &= i \int_q \int_r \text{tr} \left[D_R(q+p_*) D_R(q+p_{2*}) D_R(q) V_{\psi\psi}(p_*+q, r+p_*) \right. \\
& \qquad \qquad \qquad \left. D_R(r) D_R(r+p_{4*}) D_R(r+p_*) \right], \tag{149}
\end{aligned}$$

$$\begin{aligned}
F_{VV} &= \int_k \int_q \int_r \left\{ \text{tr} \left[D_R(q+p_*) D_R(q+p_{2*}) D_R(q) V_{\psi\psi}(p_*+q, r+p_*) \right. \right. \\
& \qquad \qquad \qquad \left. \left. D_R(r) D_R(r-k) D_R(r+p_*) \right] G_R(k) G_R(k+p_*) \bar{V}^{(4)}(k+p_*, p_{3*}) \right\}. \tag{150}
\end{aligned}$$

Note that F_V and F_{VV} are both finite, and F_4 and F_{4V} are logarithmically divergent. The remaining counterterms $\delta\lambda_2$ and $\delta\alpha_1$ are obtained in the exact same manner as in the scalar sunset case, and the expressions are the same (108) and (112), with the vertex function now being defined with the modified four-point scalar kernel to include the contributions from fermions.

We can now turn to the formulation of the gap equations to determine the form of the fermionic and scalar propagators. These are given by

$$\begin{aligned}
iG_R^{-1}(p) &= p^2 - m_R^2 - i\bar{\Pi}(p) \\
&= (p^2 - m_R^2) + (\delta Z_{\phi,0} p^2 - \delta m_0^2) - (\alpha_R + \delta\alpha_1)\phi_R - \frac{(\lambda_R + \delta\lambda_2)}{2}\phi_R^2 \\
&\quad - \frac{(\lambda_R + \delta\lambda_0)}{2}\mathcal{T} + \frac{(\alpha_R + \lambda_R\phi_R)^2}{2}\mathcal{I}(p) - ig_R^2 \int_q \text{tr}[D_R(q)D_R(p+q)] \\
&\equiv (p^2 - m_R^2) + (\delta Z_{\phi,0} p^2 - \delta m_0^2) - (\alpha_R + \delta\alpha_1)\phi_R - \frac{(\lambda_R + \delta\lambda_2)}{2}\phi_R^2 \\
&\quad - \frac{(\lambda_R + \delta\lambda_0)}{2}\mathcal{T} + \frac{(\alpha_R + \lambda_R\phi_R)^2}{2}\mathcal{I}(p) - g_R^2 [p^2\mathcal{F}_1(p) + \mathcal{F}_2(p)] \quad (151)
\end{aligned}$$

$$\begin{aligned}
iD_R^{-1}(p) &= \not{p} - M_R - i\bar{\Sigma}(\not{p}) \\
&= \not{p} - M_R + (\delta Z_{\psi,0}\not{p} - \delta M_0) - (g_R + \delta g_1)\phi_R - ig_R^2 \int_q D_R(p+q)G_R(q) \\
&\equiv \not{p} - M_R + (\delta Z_{\psi,0}\not{p} - \delta M_0) - (g_R + \delta g_1)\phi_R - g_R^2 [X(p)\not{p} + Y(p)] , \quad (152)
\end{aligned}$$

and are evidently coupled. For the loop integrals related to fermions, we have decomposed them into forms based on possible Lorentz structures. We now impose the appropriate on-shell renormalization conditions to obtain the counterterms related to the propagators. For the scalar propagator, we have

$$\delta Z_{\phi,0} = -\frac{(\alpha_R + \lambda_R\phi_R)^2}{2} \frac{\partial \mathcal{I}(p)}{\partial p^2} \Big|_{p^2=m_R^2} + g_R^2 \left[\mathcal{F}_1(p) + m_R^2 \frac{\partial \mathcal{F}_1(p)}{\partial p^2} + \frac{\partial \mathcal{F}_2(p)}{\partial p^2} \right] \Big|_{p^2=m_R^2} , \quad (153)$$

$$\begin{aligned}
\delta m_0^2 &= \delta Z_{\phi,0} m_R^2 - (\alpha_R + \delta\alpha_1)\phi_R - \frac{(\lambda_R + \delta\lambda_2)}{2}\phi_R^2 - \frac{(\lambda_R + \delta\lambda_0)}{2}\mathcal{T} \\
&\quad + \frac{(\alpha_R + \lambda_R\phi_R)^2}{2}\mathcal{I}(p) \Big|_{p^2=m_R^2} - g_R^2 [m_R^2\mathcal{F}_1(p) + \mathcal{F}_2(p)] \Big|_{p^2=m_R^2} , \quad (154)
\end{aligned}$$

and for the fermionic propagator

$$\delta Z_{\psi,0} = g_R^2 X(p) \Big|_{p^2=M_R^2} + 2g_R^2 M_R \left[M_R \frac{\partial X(p)}{\partial p^2} + \frac{\partial Y(p)}{\partial p^2} \right] \Big|_{p^2=M_R^2} , \quad (155)$$

$$\delta M_0 = \delta Z_{\psi,0} M_R - (g_R + \delta g_1) \phi_R - g_R^2 [M_R X(p) + Y(p)] \Big|_{p^2=M_R^2} . \quad (156)$$

Note that the counterterms for the scalar and fermionic wave function renormalizations are not finite, due to the loop integrals not always being subtracted.

We proceed now in the same manner as in the scalar sunset approximation: we substitute these counterterms into the gap equations to obtain the following coupled integral equations to solve for the propagators

$$\begin{aligned} iG_R^{-1}(p) &= (p^2 - m_R^2) \left[1 - \frac{(\alpha_R + \lambda_R \phi_R)^2}{2} \frac{\partial \mathcal{I}(q)}{\partial q^2} + g_R^2 \left(m_R^2 \frac{\partial \mathcal{F}_1(q)}{\partial q^2} + \frac{\partial \mathcal{F}_1(q)}{\partial q^2} \right) \right] \Big|_{q^2=m_R^2} \\ &+ \frac{(\alpha_R + \lambda_R \phi_R)^2}{2} \left[\mathcal{I}(p) - \mathcal{I}(q) \Big|_{q^2=m_R^2} \right] \\ &- g_R^2 \left[p^2 \left(\mathcal{F}_1(p) - \mathcal{F}_1(q) \Big|_{q^2=m_R^2} \right) + \left(\mathcal{F}_2(p) - \mathcal{F}_2(q) \Big|_{q^2=m_R^2} \right) \right] , \end{aligned} \quad (157)$$

$$\begin{aligned} iD_R^{-1}(p) &= (\not{p} - M_R) \left[1 + 2g_R^2 M_R \left(M_R \frac{\partial X(q)}{\partial q^2} + \frac{\partial Y(q)}{\partial q^2} \right) \right] \Big|_{q^2=M_R^2} \\ &- g_R^2 \left[\not{p} \left(X(p) - X(q) \Big|_{q^2=M_R^2} \right) + \left(Y(p^2) - Y(q) \Big|_{q^2=M_R^2} \right) \right] \\ &\equiv W(p) \not{p} - Z(p) . \end{aligned} \quad (158)$$

These are manifestly finite as divergences drop out due to the subtraction from a fixed point or differentiation of the divergent functions. In the last step for the fermionic propagator, we have defined the following quantities

$$W(p) = 1 - g_R^2 \left(X(p) - X(q) \Big|_{q^2=M_R^2} \right) + 2g_R^2 M_R \left(M_R \frac{\partial X(q)}{\partial q^2} + \frac{\partial Y(q)}{\partial q^2} \right) \Big|_{q^2=M_R^2} , \quad (159)$$

$$Z(p) = M_R - g_R^2 \left(Y(p) - Y(q) \Big|_{q^2=M_R^2} \right) - 2g_R^2 M_R^2 \left(M_R \frac{\partial X(q)}{\partial q^2} + \frac{\partial Y(q)}{\partial q^2} \right) \Big|_{q^2=M_R^2} , \quad (160)$$

according to which we can explicitly write down the expressions for $X(p)$ and $Y(p)$,

$$X(p) = i \int_q W(p+q) G_R(q) , \quad Y(p) = i \int_q Z(p+q) G_R(q) . \quad (161)$$

For the trace that appears in the scalar propagator, we resolve this as

$$\text{tr}[D_R(q) D_R(p+q)] = \text{tr} \left\{ \frac{i}{W(q) \not{q} - Z(q)} \frac{i}{W(p+q) (\not{p} + \not{q}) - Z(p+q)} \right\}$$

$$\begin{aligned}
&= \frac{\text{tr} \{ [W(q)\not{q} + Z(q)][W(p+q)(\not{p} + \not{q}) + Z(p+q)] \}}{[W^2(q)q^2 - Z^2(q)][W^2(p+q)(p+q)^2 - Z^2(p+q)]} \\
&= 4 \frac{(p \cdot q + q^2)W(q)W(p+q) + Z(q)Z(p+q)}{[W^2(q)q^2 - Z^2(q)][W^2(p+q)(p+q)^2 - Z^2(p+q)]} \\
&= p^2 \left\{ \frac{-2W(q)W(p+q)}{[W^2(q)q^2 - Z^2(q)][W^2(p+q)(p+q)^2 - Z^2(p+q)]} \right\} \\
&\quad + 2 \left\{ \frac{((p+q)^2 - q^2)W(q)W(p+q) + Z(q)Z(p+q)}{[W^2(q)q^2 - Z^2(q)][W^2(p+q)(p+q)^2 - Z^2(p+q)]} \right\} \tag{162}
\end{aligned}$$

where in the second last step we have used $2p \cdot q = (p+q)^2 - p^2 - q^2$. This finally gives the expressions for the functions \mathcal{F}_1 and \mathcal{F}_2

$$\mathcal{F}_1(p) = -2i \int_q \frac{W(q)W(p+q)}{[W^2(q)q^2 - Z^2(q)][W^2(p+q)(p+q)^2 - Z^2(p+q)]}, \tag{163}$$

$$\mathcal{F}_2(p) = 2i \int_q \frac{((p+q)^2 - q^2)W(q)W(p+q) + Z(q)Z(p+q)}{[W^2(q)q^2 - Z^2(q)][W^2(p+q)(p+q)^2 - Z^2(p+q)]}. \tag{164}$$

We now have the entire setup to solve the gap equations, which we approach in the same iterative manner outlined for the scalar sunset approximation, beginning with the free propagators. This yields

$$X^{(1)}(p^2) = \frac{1}{16\pi^2} [B_1(p^2, m_R^2, M_R^2) + B_0(p^2, m_R^2, M_R^2)], \tag{165}$$

$$Y^{(1)}(p^2) = \frac{1}{16\pi^2} [M_R B_0(p^2, m_R^2, M_R^2)], \tag{166}$$

$$\begin{aligned}
i(G_R^{-1}(p))^{(1)} &= p^2 \left\{ 1 - \frac{g_R^2}{8\pi^2} [B_0(p^2, M_R^2, M_R^2) - B_0(m_R^2, M_R^2, M_R^2)] \right. \\
&\quad \left. - \frac{g_R^2}{4\pi^2} \left(M_R^2 - \frac{m_R^2}{2} \right) \dot{B}_0(m_R^2, M_R^2, M_R^2) - \frac{(\alpha_R + \lambda_R \phi_R)^2}{32\pi^2} \dot{B}_0(m_R^2, m_R^2, m_R^2) \right\} \\
&- m_R^2 \left\{ 1 - \frac{g_R^2}{8\pi^2} \frac{M_R^2}{m_R^2} [B_0(p^2, M_R^2, M_R^2) - B_0(m_R^2, M_R^2, M_R^2)] \right. \\
&\quad \left. - \frac{g_R^2}{4\pi^2} \left(M_R^2 - \frac{m_R^2}{2} \right) \dot{B}_0(m_R^2, M_R^2, M_R^2) + \frac{(\alpha_R + \lambda_R \phi_R)^2}{32\pi^2} \dot{B}_0(m_R^2, m_R^2, m_R^2) \right\} \\
&\quad + \frac{(\alpha_R + \lambda_R \phi_R)^2}{32\pi^2} [B_0(p^2, m_R^2, m_R^2) - B_0(m_R^2, m_R^2, m_R^2)], \tag{167}
\end{aligned}$$

which are converted to Euclidean space for the next iteration. We focus on the case of a large Yukawa coupling, $g_R = 2$, and set smaller couplings pertaining to scalars. We again

see that the relative difference between successive iterations drops by about two orders of magnitude for the scalar propagator (Fig. 6) and the functions $W(p)$ (Fig. 7) and $Z(p)$ (Fig. 8), demonstrating the convergence of this approach. The spikes correspond to cases where the corresponding difference vanishes.

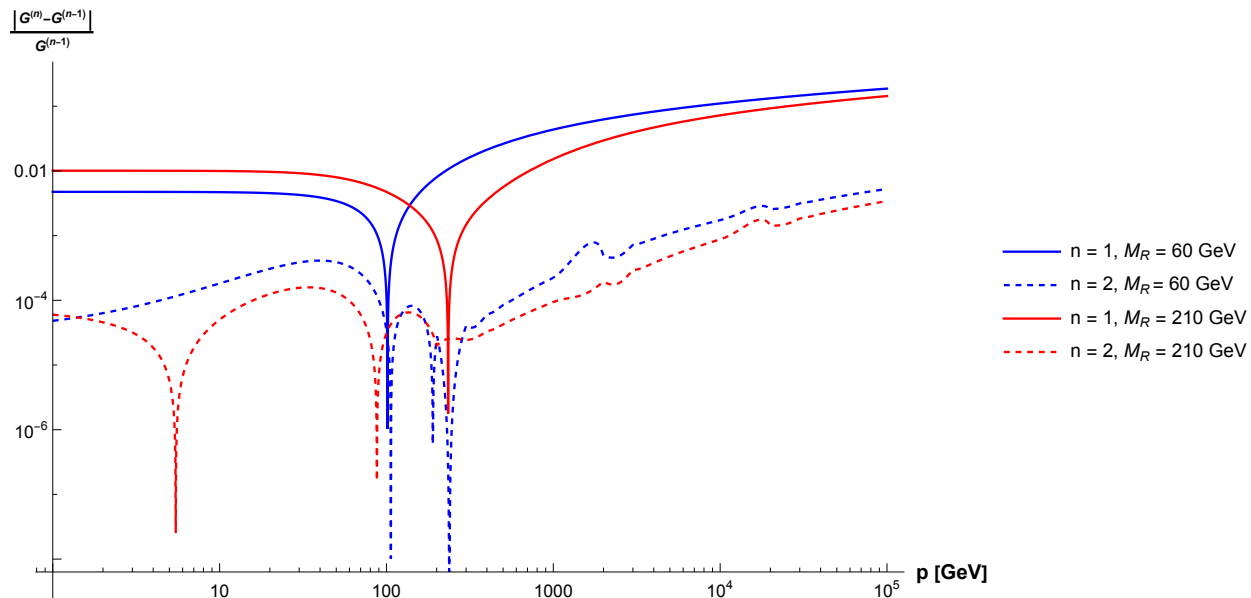


Figure 6: The relative difference between the two successive iterations of the scalar propagator for two choices of the renormalised fermionic mass, M_R . We have set $g_R = 2$, $\lambda_R = 0.5$, $\alpha_R = 50$ GeV, $\phi_R \approx 227.5$ GeV and $m_R = 100$ GeV in all cases. The UV cutoff was taken to be $\Lambda = 10^5$ GeV.

We now outline the procedure to obtain the remaining counterterms, which pertain to the scalar field. We must start with the generic expression involving field derivatives of the effective action and include the relevant modifications due to the presence of fermions.

Starting with the scalar one-point function, we have

$$\begin{aligned} \frac{\delta\Gamma^{2\text{PI}}}{\delta\phi_R(x_1)} &= \left. \frac{\delta\Gamma^{2\text{PI}}}{\delta\phi_R(x_1)} \right|_{\phi_R, G_R, D_R} + \int_{y_1, y_2} \left. \frac{\delta\Gamma^{2\text{PI}}}{\delta G_R(y_1, y_2)} \right|_{\phi_R, G_R, D_R} \frac{\delta G_R(y_1, y_2)}{\delta\phi_R(x_1)} \\ &\quad + \int_{y_1, y_2} \text{tr} \left\{ \left. \frac{\delta\Gamma^{2\text{PI}}}{\delta D_R(y_1, y_2)} \right|_{\phi_R, G_R, D_R} \frac{\delta D_R(y_1, y_2)}{\delta\phi_R(x_1)} \right\} \end{aligned}$$

where the second and third terms are obtained from the chain rule. The stationarity conditions of $\Gamma^{2\text{PI}}$,

$$\left. \frac{\delta\Gamma^{2\text{PI}}}{\delta G_R} \right|_{\phi_R, G_R, D_R} = \left. \frac{\delta\Gamma_{2\text{PI}}}{\delta D_R} \right|_{\phi_R, G_R, D_R} \stackrel{!}{=} 0, \quad (168)$$

cause these to drop out. We thus obtain, by converting to momentum space,

$$\Gamma^{(1)} = \left. \frac{\delta\Gamma^{2\text{PI}}}{\delta\phi_R} \right|_{p^2=0} = -\delta t_1 - (m_R^2 + \delta m_2^2)\phi_R - \frac{(\alpha_R + \delta\alpha_3)}{2}\phi_R^2 - \frac{(\lambda_R + \delta\lambda_4)}{6}\phi_R^3$$

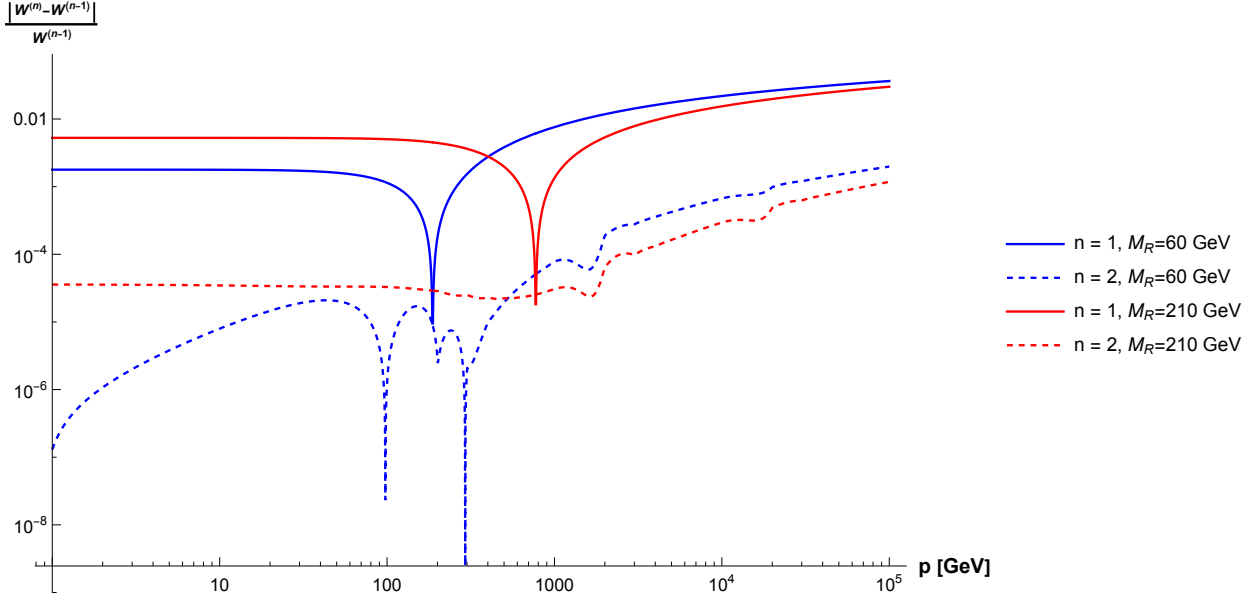


Figure 7: The relative difference between the two successive iterations of the function $W(p)$ for two choices of the renormalised fermionic mass, M_R . All parameters are set as in Fig. 6.

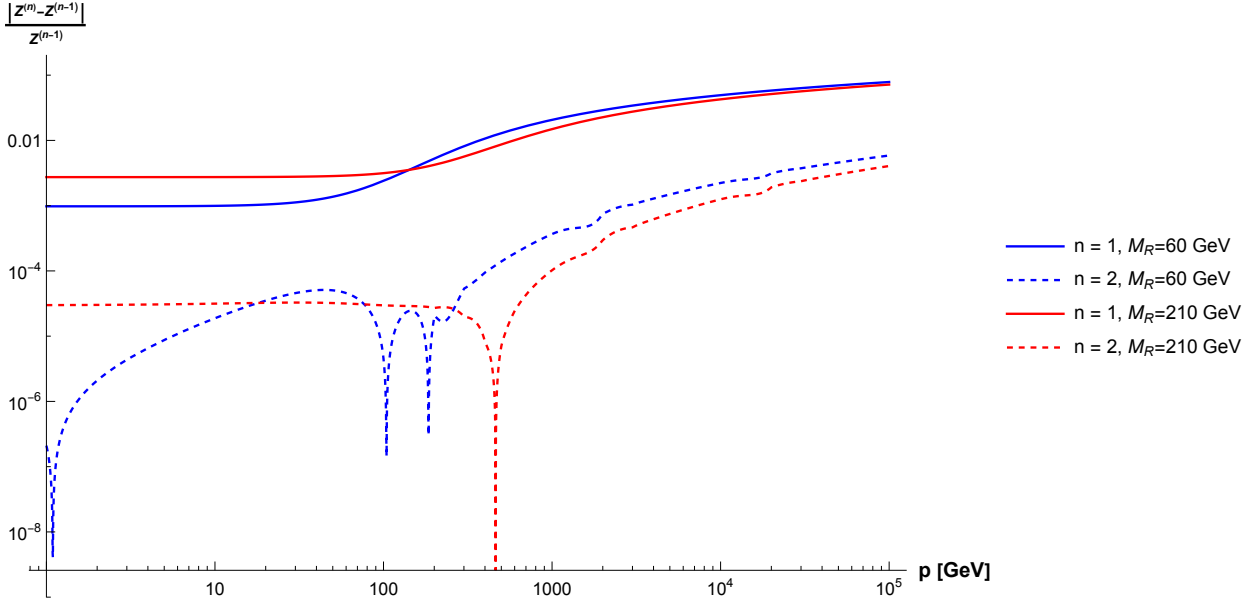


Figure 8: The relative difference between the two successive iterations of the function $Z(p)$ for two choices of the renormalised fermionic mass, M_R . All parameters are set as in Fig. 6.

$$-\frac{1}{2} [(\alpha_R + \delta\alpha_1) + (\lambda_R + \delta\lambda_2)\phi_R] \mathcal{T} + \frac{\lambda_R(\alpha_R + \lambda_R\phi_R)}{6} \mathcal{S} - (g_R + \delta g_1) \int_q \text{tr} [D_R(q)] \stackrel{!}{=} 0, \quad (169)$$

which is the same minimisation condition as in the scalar sunset, but with a new contribution

from the fermionic tadpole, which is the last term in the second line.

Consider the physical two-point function of the scalar field,

$$\begin{aligned}
\Gamma^{(2)}(x_1, x_2) &\equiv \frac{\delta^2 \Gamma^{2\text{PI}}}{\delta\phi(x_1)\delta\phi(x_2)} \\
&= \frac{\delta^2 \Gamma^{2\text{PI}}}{\delta\phi_R(x_1)\delta\phi_R(x_2)} \Big|_{\phi_R, G_R, D_R} + \int_{y_1, \dots, y_4} \frac{\delta^2 \Gamma^{2\text{PI}}}{\delta\phi_R(x_1)\delta G_R(y_1, y_2)} \Big|_{\phi_R, G_R, D_R} \frac{\delta G_R(y_1, y_2)}{\delta\phi_R(x_2)} \\
&\quad + \int_{y_1, \dots, y_4} \text{tr} \left\{ \frac{\delta^2 \Gamma^{2\text{PI}}}{\delta\phi(x_1)\delta D_R(y_1, y_2)} \Big|_{\phi_R, G_R, D_R} \frac{\delta D_R(y_1, y_2)}{\delta\phi_R(x_2)} \right\} \\
&= iG_{0,R}^{-1} + \frac{\delta^2 \Gamma_{\text{int}}^{2\text{PI}}}{\delta\phi_R(x_1)\delta\phi_R(x_2)} \Big|_{\phi_R, G_R, D_R} \\
&\quad + \int_{y_1, \dots, y_4} \frac{\delta^2 \Gamma_{\text{int}}^{2\text{PI}}}{\delta\phi_R(x_1)\delta G_R(y_1, y_2)} \Big|_{\phi_R, G_R, D_R} G_R(y_1, y_3) \frac{\delta \bar{\Pi}(y_3, y_4)}{\delta\phi_R(x_2)} G_R(y_4, y_2) \\
&\quad + \int_{y_1, \dots, y_4} \text{tr} \left\{ \frac{\delta^2 \Gamma_{\text{int}}^{2\text{PI}}}{\delta\phi_R(x_1)\delta D_R(y_1, y_2)} \Big|_{\phi_R, G_R, D_R} D_R(y_1, y_3) \frac{\delta \bar{\Sigma}(y_3, y_4)}{\delta\phi_R(x_2)} D_R(y_4, y_2) \right\}.
\end{aligned} \tag{170}$$

The last line gives explicit fermionic contributions by virtue of $\delta \bar{\Sigma} / \delta \phi_R$. In a similar manner to (81), it can be expanded out using the following diagrammatic equation

$$\frac{\delta \bar{\Sigma}(x_1, x_2)}{\delta\phi_R(x_3)} \equiv \frac{1}{2} \text{---} \square \text{---} \circ 3 = \frac{1}{2} \text{---} \bullet \text{---} \circ 3 + \frac{1}{2} \text{---} \boxed{V_{\psi\psi}} \text{---} \bullet \text{---} \circ 3 + \frac{1}{2} \text{---} \boxed{V_{\psi\phi}^{(4)}} \text{---} \bullet \text{---} \circ 3 \tag{171}$$

where we have the new building blocks involving fermions. cyan lines indicate fermionic propagators. Note the appearance of the vertex functions $V_{\psi\psi}$ and $V_{\psi\phi}$ now, which appear as a solution to the self-energy equation of $\delta \bar{\Sigma} / \delta \phi_R$, in the similar manner how $\bar{V}^{(4)}$ appeared as solution to $\delta \bar{\Pi} / \delta \phi_R$. We stress that the $\bar{V}^{(4)}$ used is (145) with the modified four-point scalar kernel. Furthermore, note that correspondingly $\delta \bar{\Pi} / \delta \phi_R$ is modified from (81) and gains the additional part

$$\frac{1}{2} \text{---} \square \text{---} \circ 3 = \frac{1}{2} \text{---} \bullet \text{---} \circ 3 + \frac{1}{2} \text{---} \boxed{\bar{V}^{(4)}} \text{---} \bullet \text{---} \circ 3 + \frac{1}{2} \text{---} \boxed{V_{\phi\psi}^{(4)}} \text{---} \bullet \text{---} \circ 3 \tag{172}$$

where $V_{\phi\psi}^{(4)}$ is the transpose of the vertex function $V_{\psi\phi}^{(4)}$. We continue now with the diagrammatic analysis and look at the 3-point and 4-point functions, required to obtain the counterterms $\delta\alpha_3$ and $\delta\lambda_4$. Besides the scalar contributions in (126) and (127), we have in

addition the following ones from the fermions

$$\Gamma^{(3)} \Big|_{\text{fermions}} = \begin{array}{c} \text{---} \bullet \text{---} \square \text{---} \text{---} \\ | \\ \square \\ | \\ \circ \end{array} + \begin{array}{c} \text{---} \bullet \text{---} \square \text{---} \text{---} \\ | \\ \square \\ | \\ \circ \end{array}, \quad (173)$$

$$\Gamma^{(4)} \Big|_{\text{fermions}} = \begin{array}{c} \circ \\ | \\ \square \\ | \\ \bullet \\ | \\ \square \\ | \\ \circ \end{array} + \begin{array}{c} \circ \\ | \\ \square \\ | \\ \bullet \\ | \\ \square \\ | \\ \circ \end{array} + \begin{array}{c} \circ \\ | \\ \bullet \text{---} \square \text{---} \text{---} \\ | \\ \square \\ | \\ \circ \end{array}. \quad (174)$$

A factor of $\frac{1}{2}$ does not appear for the fermionic self-energy insertions as this quantity is not defined with a factor of 2 (compare (13) and (16)). Now, we list the non-vanishing fermionic contributions to the derivatives of the scalar self-energy which would be inserted in to the above equations

$$\begin{array}{c} \square \\ | \\ \circ \end{array} \Big|_{\text{fermions}} = + \begin{array}{c} \square \text{---} \bullet \text{---} \square \text{---} \text{---} \\ | \\ \square \\ | \\ \circ \end{array} + \begin{array}{c} \square \text{---} V_{\phi\psi}^{(4)} \text{---} \bullet \text{---} \square \text{---} \text{---} \\ | \\ \square \\ | \\ \circ \end{array} \quad (175)$$

$$\begin{array}{c} \square \\ | \\ \circ \end{array} \Big|_{\text{fermions}} = \begin{array}{c} \circ \\ | \\ \square \\ | \\ \bullet \\ | \\ \square \\ | \\ \circ \end{array} + \begin{array}{c} \circ \\ | \\ \square \\ | \\ \bullet \\ | \\ \square \\ | \\ \circ \end{array} + \begin{array}{c} \square \text{---} \bullet \text{---} \square \text{---} \text{---} \\ | \\ \square \\ | \\ \circ \end{array} + \begin{array}{c} \square \text{---} V_{\phi\psi}^{(4)} \text{---} \bullet \text{---} \square \text{---} \text{---} \\ | \\ \square \\ | \\ \circ \end{array}, \quad (176)$$

and finally, those of the fermionic self-energy

$$\begin{aligned}
 \text{Diagram} &= \text{Diagram 1} + \text{Diagram 2} + \text{Diagram 3}
 \end{aligned}
 \tag{177}$$

$$\begin{aligned}
 \text{Diagram} &= \text{Diagram 1} + \text{Diagram 2} + \text{Diagram 3}
 \end{aligned}
 \tag{178}$$

With these, one can analyse the scalar n -point functions with fermionic contributions and obtain the field counterterms. Moreover, we note that this diagrammatic analysis extends to higher truncations of the 2PI effective action involving fermions.

6 Conclusions and Outlook

We have investigated an on-shell scheme for the 2PI formalism with a particular focus on the equations of motion, the motivation being that one can obtain from these in principle the transport equations which are relevant, for example, while studying cosmological phase transitions. After an outline of the generic procedure, we have revisited in a first step the so-called Hartree approximation as one can obtain in this case analytic formulas for all interesting quantities. We have given the relation between the counterterms in the broken and unbroken phases. Moreover, we have given the formulas for three- and four-point functions in the broken phase. A particular feature of this approximation is, that all counterterms are finite and the resummed two-point function has the same form as the tree-level one. Neither of these hold when going beyond this approximation.

In a second step, we have first allowed for an additional independent trilinear scalar coupling in the classical action which induces the so-called scalar sunset diagram at two-loop level. We have used this toy model to give the explicit procedure on how to obtain the on-shell counterterms in a more complicated system. Moreover, we have shown that the two-point function G can be evaluated numerically in a fast converging iteration. This in turn serves as input for the calculation of the renormalized three- and four-point functions.

For a Yukawa theory, the equations of motion for the scalar and fermionic two-point functions are coupled. We have demonstrated that the numerical procedure used in the

pure scalar case works also for this coupled system even for $\mathcal{O}(1)$ couplings. We have given explicitly the counterterms for the wave function and mass renormalization, whereas in the case of the coupling counterterms, we give a diagrammatic form which can easily be translated into formulae, which are however very lengthy.

The procedure outlined in this paper can easily be extended to the case of multiple scalars and fermions. It can also be extended to include gauge fields which we will discuss in a forthcoming paper. From our results, one can easily get the counterterms for other renormalization schemes such as $\overline{\text{MS}}$. This scheme is widely used for the calculation of the effective potential, which is an important tool for the study of phase transitions.

Acknowledgements

We thank K. Kainulainen and O. Koskivaara for discussions and Ch. Gross for collaboration in the early stage of this project. This work has been supported by the DFG, project nrs. PO-1337/8-1 and HI 744/10-1.

References

- [1] R. Jackiw, Phys. Rev. D **9**, 1686 (1974).
- [2] J. M. Cornwall, R. Jackiw, and E. Tomboulis, Phys. Rev. D **10**, 2428 (1974).
- [3] J. P. Blaizot, E. Iancu, and A. Rebhan, Phys. Rev. D **63**, 065003 (2001), arXiv:hep-ph/0005003.
- [4] J. O. Andersen and M. Strickland, Phys. Rev. D **71**, 025011 (2005), arXiv:hep-ph/0406163.
- [5] J. Berges, S. Borsanyi, U. Reinosa, and J. Serreau, Phys. Rev. D **71**, 105004 (2005), arXiv:hep-ph/0409123.
- [6] A. Arrizabalaga, J. Smit, and A. Tranberg, JHEP **10**, 017 (2004), arXiv:hep-ph/0409177.
- [7] E. Calzetta and B. L. Hu, Phys. Rev. D **37**, 2878 (1988).
- [8] Y. B. Ivanov, J. Knoll, and D. N. Voskresensky, Nucl. Phys. A **657**, 413 (1999), arXiv:hep-ph/9807351.
- [9] J. Berges, AIP Conf. Proc. **739**, 3 (2004), arXiv:hep-ph/0409233.
- [10] J. Berges, (2015), arXiv:1503.02907.
- [11] A. Arrizabalaga, J. Smit, and A. Tranberg, Phys. Rev. D **72**, 025014 (2005), arXiv:hep-ph/0503287.

- [12] J. Berges and S. Roth, Nucl. Phys. B **847**, 197 (2011), arXiv:1012.1212.
- [13] T. Konstandin, Phys. Usp. **56**, 747 (2013), arXiv:1302.6713.
- [14] H. Jukkala, K. Kainulainen, and O. Koskivaara, JHEP **01**, 012 (2020), arXiv:1910.10979.
- [15] T. Prokopec, M. G. Schmidt, and S. Weinstock, Annals Phys. **314**, 208 (2004), arXiv:hep-ph/0312110.
- [16] T. Prokopec, M. G. Schmidt, and S. Weinstock, Annals Phys. **314**, 267 (2004), arXiv:hep-ph/0406140.
- [17] J.-P. Blaizot, E. Iancu, and U. Reinosa, Phys. Lett. B **568**, 160 (2003), arXiv:hep-ph/0301201.
- [18] J.-P. Blaizot, E. Iancu, and U. Reinosa, Nucl. Phys. A **736**, 149 (2004), arXiv:hep-ph/0312085.
- [19] M. E. Carrington, W.-J. Fu, D. Pickering, and J. W. Pulver, Phys. Rev. D **91**, 025003 (2015), arXiv:1404.0710.
- [20] M. E. Carrington *et al.*, Phys. Rev. D **97**, 036005 (2018), arXiv:1711.09135.
- [21] A. Patkos and Z. Szep, Nucl. Phys. A **811**, 329 (2008), arXiv:0806.2554.
- [22] A. Patkos and Z. Szep, Nucl. Phys. A **820**, 255C (2009), arXiv:0809.3551.
- [23] A. Pilaftsis and D. Teresi, Nucl. Phys. B **874**, 594 (2013), arXiv:1305.3221.
- [24] A. Pilaftsis and D. Teresi, J. Phys. Conf. Ser. **631**, 012008 (2015), arXiv:1502.07986.
- [25] A. Pilaftsis and D. Teresi, Nucl. Phys. B **920**, 298 (2017), arXiv:1703.02079.
- [26] U. Reinosa and J. Serreau, JHEP **07**, 028 (2006), arXiv:hep-th/0605023.
- [27] U. Reinosa and J. Serreau, JHEP **11**, 097 (2007), arXiv:0708.0971.
- [28] U. Reinosa and J. Serreau, Annals Phys. **325**, 969 (2010), arXiv:0906.2881.
- [29] O. Oliveira and R. C. Terin, (2022), arXiv:2204.04197.
- [30] U. Reinosa, Nucl. Phys. A **772**, 138 (2006), arXiv:hep-ph/0510119.
- [31] J. Berges, S. Borsanyi, U. Reinosa, and J. Serreau, Annals Phys. **320**, 344 (2005), arXiv:hep-ph/0503240.
- [32] N. N. Bogoliubow and O. S. Parasiuk, Acta Mathematica **97**, 227 (1957).
- [33] K. Hepp, Commun. Math. Phys. **2**, 301 (1966).

- [34] W. Zimmermann, Commun. Math. Phys. **15**, 208 (1969).
- [35] S. Weinberg, Phys. Rev. **118**, 838 (1960).
- [36] A. Denner, Fortsch. Phys. **41**, 307 (1993), arXiv:0709.1075.
- [37] K. Kainulainen and O. Koskivaara, JHEP **12**, 190 (2021), arXiv:2105.09598.